

State-Space Based Approach to Particle Creation in Spatially Uniform Electric Fields

Carl E. Dolby and Stephen F. Gull

*Astrophysics Group, Cavendish Laboratory, Madingley Road, Cambridge CB3 0HE,
U.K.*

E-mail: c.dolby@mrao.cam.ac.uk

Our formalism described recently in [13] is applied to the study of particle creation in spatially uniform electric fields, concentrating on the cases of a time-invariant electric field and a so-called ‘adiabatic’ electric field. Several problems are resolved by incorporating the ‘Bogoliubov coefficient’ approach and the ‘tunnelling’ approaches into a single consistent, gauge invariant formulation. The value of a time-dependent particle interpretation is demonstrated by presenting a coherent account of the time-development of the particle creation process, in which the particles are created with small momentum (in the frame of the electric field) and are then accelerated by the electric field to make up the ‘bulge’ of created particles predicted by asymptotic calculations [2]. An initial state comprising one particle is also considered, and its evolution is described as being the sum of two contributions: the ‘sea of current’ produced by the evolved vacuum, and the extra current arising from the initial particle state.

Key Words: particle creation, fermion, Slater determinant.

1. INTRODUCTION

It has long been known that a strong classical electromagnetic background can cause vacuum instability and generate particle/antiparticle pairs. This phenomenon was first studied in 1951 by Schwinger [1], who predicted particle creation in a constant electric field. Schwinger’s predictions were based on the imaginary component of the effective action, but the same result has since been derived from a variety of alternative approaches: Bogoliubov coefficients within a Canonical formalism [2], tunnelling amplitudes [3, 4, 5], a wave-functional method [6, 7], and particle detectors [8, 9]. (In [10, 11] back-reaction is also considered.) A brief review is presented by Sriramkumar et al. [8], who point out that the predictions of these approaches do not always agree. The same authors

point out in [12] that approaches based on Bogoliubov coefficients or on tunnelling amplitudes are liable to suffer from a gauge-dependent particle definition (i.e., choice of ‘in’ and ‘out’ modes) which can in turn lead to gauge-dependent predictions of the number of particles created.

We have recently introduced an alternative approach to the study of particle creation in electromagnetic backgrounds [13] which uses methods analogous to those of conventional multiparticle quantum mechanics. Our approach is to emphasise the states of the system, described in terms of Slater determinants of Dirac states. The vacuum state ‘at time τ ’ is described in terms of the Slater determinant of all ‘negative energy’ states, and provides a concrete realisation of the Dirac Sea. This approach has provided straightforward derivations of the general S-Matrix element and expectation value of the theory, using only methods familiar from multiparticle quantum mechanics. We argued in [13] that this approach is often quicker and clearer than conventional methods. More importantly, the ‘Bogoliubov coefficient’ and ‘tunnelling amplitude’ methods were combined consistently into a single gauge invariant formulation, which could be linked to the motion of an observer (detector).

As with the Canonical, Tunnelling, and Wave-functional approaches, our analysis depends explicitly on a choice of ‘in’ and ‘out’ particle interpretation, and on the corresponding categorisation of in and out modes. Various categorisation schemes have been proposed, based on asymptotic or adiabatic properties of solutions, or on the diagonalisation of a suitable Hamiltonian. Unfortunately, most schemes depend on a choice of coordinates (as in the Unruh effect [20]) or of gauge [12], and the relation of these to the behaviour of a particle detector is often ambiguous [8]. Also, those schemes based on asymptotic or adiabatic approximations generate accurate predictions only at asymptotically late times or in sufficiently weak electromagnetic backgrounds. Particle detectors provide a more operational particle concept, but their predictions are not always proportional to the number of particles present [8, 9] even when the detector is inertial.

The categorisation scheme suggested in [13] provides a consistent particle interpretation at all times without requiring any asymptotic conditions on the in and out states. It consistently combines the conventional ‘Bogoliubov coefficient’ and ‘tunnelling amplitude’ methods, resolving gauge inconsistencies that trouble each of these [12]. Also, by utilising the concept of radar time, this definition naturally incorporates the motion of the observer (detector), providing a definition which depends only on the observer’s motion and on the background, and not on the choice of coordinates or gauge.

The present paper presents a simple application of this formulation. We shall examine the problem of pair creation in time-varying spatially uniform electric fields, as viewed by an observer stationary with respect to

this electric field. We present definite results for a constant electric field $\mathbf{E}(t) = (0, 0, E)$ and for the so-called ‘adiabatic’ [2] electric field $\mathbf{E}(t) = (0, 0, E \operatorname{sech}^2(mt/\rho))$. Such backgrounds have been studied by various authors [1, 7, 5, 4], who derived pair-creation rates as time-averages over an infinite period of time. The problem of pair creation after a finite evolution time has only recently been considered only recently [6, 2]. The electric field was taken as constant within a certain time interval (say $0 < t < T$), but was zero before and after. The ‘in’ and ‘out’ states were defined in the ‘free regions’ before the field was turned on ($t < 0$), and after it was turned off ($t > T$), where the solutions were simple plane wave states. Dependence of the results on T was then studied.

We use the particle definition proposed in [13] to consider the background $\mathbf{E} = (0, 0, E)$ for all time, and derive the magnitude of pair creation in a state which has evolved from the vacuum for a finite length of time. That is, we answer the question, “Suppose the system is in the vacuum state at some time t_0 . What will be the properties of the system at time $t_0 + T$?” We demonstrate the consistency of this particle definition, by obtaining the same answers to this question as in [2, 6]. (Although the difference between these two questions is purely formal in this case, it becomes vital when considering gravitational fields, which cannot simply be switched off whilst making measurements.) The finite time behaviour of particle creation in the ‘adiabatic’ background is also studied here, providing a consistent account of the time-dependence of this creation process. We also consider the time-development of initial states containing particles.

Section 2 is a short review of the approach to pair creation described in [13, 14]. It includes the particle definition appropriate for inertial observers, and a brief derivation of the general S-Matrix element and expectation value in terms of ‘Bogoliubov coefficients’. Section 3 is devoted to calculating the finite time Bogoliubov coefficients in an spatially uniform, time-varying electric field in terms of the solution of a simple linear, second order equation. In Section 4 we solve this equation in the case of a constant electric field, and use the result to find the number density of created pairs, and also their current density, after a finite evolution time. Section 5 presents a similar treatment for the ‘adiabatic’ electric field $\mathbf{E}(t) = (0, 0, E \operatorname{sech}^2(\frac{mt}{\rho}))$. Conclusions are set out in Section 6.

2. BACKGROUND

Let $\mathcal{H} \equiv L^2(\mathbb{R}^3)^4$ (the space of finite-norm spinor-valued functions of space) be the space of ‘first quantized’ states. The *antisymmetric Fock Hilbert space* over \mathcal{H} , denoted $\mathcal{F}_\wedge(\mathcal{H}) \equiv \bigoplus_{n=0}^\infty \wedge^n \mathcal{H}$, is the space of superpositions of all possible Slater determinants of first quantized states. The

time-dependent ‘first quantized’ Hamiltonian $\hat{H}_1(t) : \mathcal{H} \rightarrow \mathcal{H}$ is defined by:

$$\hat{H}_1(t)\psi(\mathbf{x}, t) = \left(-i \sum_{k=1}^3 \bar{\sigma}_k \nabla_k + m\gamma^0 \right) \psi(\mathbf{x}, t) \quad (1)$$

where $\bar{\sigma}_k \equiv \gamma^0 \gamma^k = \gamma_k \gamma_0$ and $\nabla_\mu \psi(x) \equiv \partial_\mu \psi(x) + ieA_\mu(x)\psi(x)$. The Dirac equation can be written in terms of this Hamiltonian as $i\nabla_0 \psi(\mathbf{x}, t) = \hat{H}_1(t)\psi(\mathbf{x}, t)$. Its expectation value is the spatial integral of the ‘00-component’ of the energy-momentum tensor:

$$\langle \psi(t_0) | \hat{H}_1(t_0) | \psi(t_0) \rangle \equiv \int_{t=t_0} d^3\mathbf{x} T^0_0(\psi(x))$$

We can use $\hat{H}_1(t_0)$ to split \mathcal{H} into $\mathcal{H} = \mathcal{H}^+(t_0) \oplus \mathcal{H}^-(t_0)$ where:

$\mathcal{H}^+(t_0)$ is the span of the positive spectrum of $\hat{H}_1(t_0)$

$\mathcal{H}^-(t_0)$ is the span of the negative spectrum of $\hat{H}_1(t_0)$

$\mathcal{H}^+(t_0)$ is the set of all positive energy states, and $\mathcal{H}^-(t_0)$ is the set of all negative energy states, as defined in the background $A_\mu(t_0)$ at time t_0 . In the Canonical formalism this definition would correspond to ‘Hamiltonian diagonalisation’ [15, 16, 17, 18] of the second-quantized Hamiltonian

$$\hat{H}(t_0) \equiv \int_{t=t_0} d^3\mathbf{x} T^0_0(\hat{\psi}(x)) ,$$

where $\hat{\psi}(x)$ is the field operator. In the past, Hamiltonian diagonalisation has been criticised [19] for its reliance on an apparently arbitrary choice of hypersurface Σ_{t_0} , (given by $t = t_0$ here) and time-translation vector field k^μ ($= \delta_0^\mu$ here). This arbitrariness has been a particularly difficult problem when considering QFT in a gravitational background, but the difficulty can be satisfactorily resolved [13, 14] by specifying Σ_{τ_0} and k^μ in terms of the worldline of the observer (or particle detector). The choice $t = t_0$, $k^\mu = \delta_0^\mu$ then emerges uniquely as appropriate to an inertial observer stationary in the frame of the electric field. When restricted to this frame, this definition is also similar to that of Fradkin et al. [21] or Greiner et al. [22]. However, in [21, 22] the Hamiltonian is taken to be $\hat{H}'(t) = \hat{H}_1(t) + eA_\mu(\mathbf{x}, t)$ so that the Dirac equation becomes $i\partial_t \psi(\mathbf{x}, t) = \hat{H}'(t)\psi(\mathbf{x}, t)$. Sriramkumar and Padmanabhan [12] pointed out that this leads to a particle definition which is gauge dependent. This problem, which has plagued previous ‘Bogoliubov coefficient’ approaches to particle creation, is usually patched up by appealing to the tunnelling interpretation: if a gauge $A = (A(\mathbf{x}), 0, 0, 0)$ is chosen,

particle creation is described in terms of particles ‘tunnelling through the barrier that separates particle/antiparticle states’ (see [3, 22] or [5] for a description of these methods). This leads to two theories, each succeeding where the other fails [12]. This is not the case here, however, since we use eigenstates of the gauge-covariant Hamiltonian $\hat{H}_1(t_0)$ to define particle states. It will emerge that particle creation in the background $A^\mu(x)$ requires either: 1) that $A^0(x) \neq 0$, so that $A^0(x)$ can act as a potential, w.r.t. which tunnelling may occur, or 2) $\mathbf{A}(x) = (A^1(x), A^2(x), A^3(x))$ is time-dependent, so that eigenstates of $\hat{H}_1(t)$ mix during evolution. Both effects contribute to the calculation of Bogoliubov coefficients [13, 14], and ensure their gauge invariance. An immediate consequence is that if a gauge can be chosen such that $A^0 = 0$ and \mathbf{A} is time-independent, then particle creation will not occur. That is, *time-independent magnetic fields cannot create particles*. This result agrees with Schwinger’s calculation [1] in terms of an effective Lagrangian, and successfully resolves the inconsistency problems raised by Sriramkumar and Padmanabhan [12].

Having defined $\mathcal{H}^\pm(t_0)$, we can now define the *vacuum at time t_0* , $|\text{vac}_{t_0}\rangle$, to be the Slater determinant of any basis of $\mathcal{H}^-(t_0)$ (normalised so that $\langle \text{vac}_{t_0} | \text{vac}_{t_0} \rangle = 1$). This specifies $|\text{vac}_{t_0}\rangle$ up to an arbitrary phase factor. It is the state in which all negative energy degrees of freedom are full, and hence is a concrete manifestation of the Dirac Sea.

To illustrate this, let $\{u_{i,t_0}; i \in I\}$, $\{v_{i,t_0}; i \in I\}$ be orthonormal bases for $\mathcal{H}^+(t_0)$ and $\mathcal{H}^-(t_0)$ respectively, where I is some index set, assumed countable for convenience (the uncountable case introduces no complications). The vacuum at time t_0 can be written as:

$$|\text{vac}_{t_0}\rangle = v_{1,t_0} \wedge v_{2,t_0} \wedge \dots \quad (2)$$

and is independent of the choice of basis for $\mathcal{H}^-(t_0)$ (up to a phase factor) because of the complete antisymmetry of the Slater determinant. The vacuum at some time $t_1 > t_0$ is:

$$|\text{vac}_{t_1}\rangle = v_{1,t_1} \wedge v_{2,t_1} \wedge \dots \quad (3)$$

By considering fermionic QFT ‘in a background’ we are ignoring direct electron-electron interactions, so that the evolved state $|\text{vac}_{t_0}(t_1)\rangle$ obtained by evolving $|\text{vac}_{t_0}\rangle$ from time t_0 to time t_1 is simply:

$$|\text{vac}_{t_0}(t_1)\rangle = v_{1,t_0}(t_1) \wedge v_{2,t_0}(t_1) \wedge \dots \quad (4)$$

where $v_{i,t_0}(t_1)$ denotes the state obtained from v_{i,t_0} by evolution to time t_1 , and will not, in general, be contained in $\mathcal{H}^-(t_1)$. We will often refer

to this state as the ‘evolved vacuum’, although it is not in fact a vacuum state.

Since the inner product of Slater determinants is simply the determinant of the ‘first quantized’ inner products, the vacuum-vacuum S-matrix element is simply:

$$\langle \text{vac}_{t_1} | \text{vac}_{t_0}(t_1) \rangle = \det[\langle v_{i,t_1} | v_{j,t_0}(t_1) \rangle] \quad (5)$$

The probability that $|\text{vac}_{t_0}(t_1)\rangle$ will be vacuum at time t_1 is then $\mathcal{P}_{\text{vac} \rightarrow \text{vac}} = |\langle \text{vac}_{t_1} | \text{vac}_{t_0}(t_1) \rangle|^2$. Although once a particle interpretation is specified this result can be derived by a number of methods [21, 7, 23], we believe that the derivation presented here (and in [13, 14]) is the shortest and clearest.

Similarly, the general S-matrix element can be written as:

$$\begin{aligned} & \langle \binom{i'_1 i'_2 \dots i'_{m'}}{j'_1 j'_2 \dots j'_{n'}}_{t_1} | \binom{i_1 i_2 \dots i_m}{j_1 j_2 \dots j_n}_{t_0} (t_1) \rangle \\ &= (-)^{J-J'} \det \left[\begin{array}{c} \begin{bmatrix} \alpha_{i'_1 i_1} & \dots & \alpha_{i'_1 i_m} \\ \vdots & & \vdots \\ \alpha_{i'_{m'} i_1} & \dots & \alpha_{i'_{m'} i_m} \end{bmatrix} \\ \begin{bmatrix} \gamma_{1 i_1} & \dots & \gamma_{1 i_m} \\ \vdots & & \vdots \\ \binom{j'_1 \dots j'_{n'}}{\text{missing}} & \dots & \binom{j'_1 \dots j'_{n'}}{\text{missing}} \end{bmatrix} \end{array} \begin{bmatrix} \beta_{i'_1 1} & \dots & \binom{j_1 \dots j_n}{\text{missing}} \\ \vdots & & \vdots \\ \beta_{i'_{m'} 1} & \dots & \binom{j_1 \dots j_n}{\text{missing}} \\ \epsilon_{11} & \dots & \binom{j_1 \dots j_n}{\text{missing}} \\ \vdots & & \vdots \\ \binom{j'_1 \dots j'_{n'}}{\text{missing}} \end{bmatrix} \right] \quad (6) \end{aligned}$$

(if $m - n = m' - n'$, and zero otherwise) where

$$\alpha_{ij}(t_1, t_0) = \langle u_{i,t_1} | u_{j,t_0}(t_1) \rangle \quad \gamma_{ij}(t_1, t_0) = \langle v_{i,t_1} | u_{j,t_0}(t_1) \rangle \quad (7)$$

$$\beta_{ij}(t_1, t_0) = \langle u_{i,t_1} | v_{j,t_0}(t_1) \rangle \quad \epsilon_{ij}(t_1, t_0) = \langle v_{i,t_1} | v_{j,t_0}(t_1) \rangle \quad (8)$$

are the *time-dependent Bogoliubov coefficients*, $(-)^{J-J'}$ is an unimportant sign convention, and $|\binom{i_1 i_2 \dots i_m}{j_1 j_2 \dots j_n}_{t_0}\rangle$ denotes a state comprised of m particles (in states $u_{i_1,t_0} \dots u_{i_m,t_0}$ with $i_1 < i_2 < \dots < i_m$ by convention), and n antiparticles (corresponding to the absence of states $v_{j_1,t_0} \dots v_{j_n,t_0}$), prepared at time t_0 .

Expectation Values

Given an operator $\hat{A}_1(t) : \mathcal{H} \rightarrow \mathcal{H}$, we can define its *physical extension* $\hat{A}_{\text{phys}}(t) : \mathcal{F}_\wedge(\mathcal{H}) \rightarrow \mathcal{F}_\wedge(\mathcal{H})$ by:

$$\hat{A}_{\text{phys}}(t) = \hat{A}_H(t) - \langle \text{vac}_t | \hat{A}_H(t) | \text{vac}_t \rangle \hat{1} \quad (9)$$

$$\text{where } \hat{A}_H : \psi_1 \wedge \psi_2 \wedge \dots \wedge \psi_N \rightarrow \sum_{i=1}^N \psi_1 \wedge \dots (\hat{A}_1 \psi_i) \wedge \psi_{i+1} \dots \wedge \psi_N \quad (10)$$

The expectation value of $\hat{A}_{\text{phys}}(t)$ in the physical vacuum at time t , $|\text{vac}_t\rangle$ is zero by construction. Its expectation value in the ‘evolved vacuum’ $|\text{vac}_{t_0}(t)\rangle$ is in general non-zero, and takes the form

$$\langle \text{vac}_{t_0}(t_1) | \hat{A}_{\text{phys}}(t_1) | \text{vac}_{t_0}(t_1) \rangle \quad (11)$$

$$= \sum_{i=1}^N \langle v_{i,t_0}(t_1) | \hat{A}_1(t_1) | v_{i,t_0}(t_1) \rangle - \sum_{i=1}^N \langle v_{i,t_1} | \hat{A}_1(t_1) | v_{i,t_1} \rangle \quad (12)$$

$$= \text{Trace}(\beta \beta^\dagger \mathbf{A}^{++} - \gamma \gamma^\dagger \mathbf{A}^{--} + \epsilon \beta^\dagger \mathbf{A}^{+-} + \beta \epsilon^\dagger \mathbf{A}^{-+}) \quad (13)$$

where we have defined:

$$\begin{aligned} \mathbf{A}_{jk}^{++} &\equiv \langle u_{j,t_1} | \hat{A}_1(t_1) | u_{k,t_1} \rangle & \mathbf{A}_{jk}^{--} &\equiv \langle v_{j,t_1} | \hat{A}_1(t_1) | v_{k,t_1} \rangle \\ \mathbf{A}_{jk}^{+-} &\equiv \langle u_{j,t_1} | \hat{A}_1(t_1) | v_{k,t_1} \rangle & \text{and } \mathbf{A}_{jk}^{-+} &\equiv \langle v_{j,t_1} | \hat{A}_1(t_1) | u_{k,t_1} \rangle \\ & & &= \overline{\mathbf{A}_{kj}^{+-}} \text{ if } \hat{A}_1 \text{ is Hermitian} \end{aligned} \quad (14)$$

The operator $\hat{N}_{\text{phys}}(t)$ that represents the number of particles (including antiparticles) present at time t is the physical extension of $\hat{N}_1(t) = \hat{P}^+(t) - \hat{P}^-(t)$, where $\hat{P}^\pm(t) : \mathcal{H} \rightarrow \mathcal{H}^\pm(t)$ are the projection operators onto $\mathcal{H}^\pm(t)$. It is easy to verify that $\hat{N}_{\text{phys}}(t_0) | \binom{i_1 i_2 \dots i_m}{j_1 j_2 \dots j_n} \rangle_{t_0} = (m+n) | \binom{i_1 i_2 \dots i_m}{j_1 j_2 \dots j_n} \rangle_{t_0}$, as required. The expectation value of $\hat{N}_{\text{phys}}(t_1)$ in the ‘evolved vacuum’ $|\text{vac}_{t_0}(t_1)\rangle$ is given (from (13)) by:

$$\begin{aligned} N_{\text{vac},t_0}(t_1) &\equiv \langle \text{vac}_{t_0}(t_1) | \hat{N}_{\text{phys}}(t_1) | \text{vac}_{t_0}(t_1) \rangle \\ &= \text{Trace}(\beta \beta^\dagger + \gamma \gamma^\dagger) \\ &= \sum_i \{ N_{i,t_0}^+(t_1) + N_{i,t_0}^-(t_1) \} \end{aligned} \quad (15)$$

where $N_{i,t_0}^+(t_1) = (\beta \beta^\dagger)_{ii}$ is the expectation value of the physical extension of $|u_{i,t_1}\rangle \langle u_{i,t_1}|$ and represents the probability that the degree of freedom u_{i,t_1} is occupied in $|\text{vac}_{t_0}(t_1)\rangle$, i.e. that particle i is present. $N_{i,t_0}^-(t_1) =$

$(\gamma\gamma^\dagger)_{ii}$ is the expectation value of the physical extension of $-|v_{i,t_1}\rangle\langle v_{i,t_1}|$; it represents the probability that the degree of freedom v_{i,t_1} is unoccupied in $|\text{vac}_{t_0}(t_1)\rangle$, i.e. that antiparticle i is present. From the unitarity of the ‘first quantized’ evolution matrix $\mathbf{S}_1(t_1, t_0) = \begin{bmatrix} \boldsymbol{\alpha}(t_1, t_0) & \boldsymbol{\beta}(t_1, t_0) \\ \boldsymbol{\gamma}(t_1, t_0) & \boldsymbol{\epsilon}(t_1, t_0) \end{bmatrix}$, it is easy to show that $\text{Trace}(\boldsymbol{\beta}\boldsymbol{\beta}^\dagger) = \text{Trace}(\boldsymbol{\gamma}\boldsymbol{\gamma}^\dagger)$, expressing charge conservation.

The derivation of $\langle F_{t_0}(t_1) | \hat{A}_{\text{phys}}(t_1) | F_{t_0}(t_1) \rangle$ for an arbitrary state $|F_{t_0}(t_1)\rangle$ is identical to the derivation of (13), and gives:

$$\begin{aligned} & \langle ({}^{i_1 i_2 \dots i_m}_{j_1 j_2 \dots j_n})_{t_0}(t_1) | \hat{A}_{\text{phys}}(t_1) | ({}^{i_1 i_2 \dots i_m}_{j_1 j_2 \dots j_n})_{t_0}(t_1) \rangle \\ &= \sum_{k=1}^m \langle u_{i_k, t_0}(t_1) | \hat{A}_1(t_1) | u_{i_k, t_0}(t_1) \rangle - \sum_{k=1}^n \langle v_{j_k, t_0}(t_1) | \hat{A}_1(t_1) | v_{j_k, t_0}(t_1) \rangle \\ & \quad + \langle \text{vac}_{t_0}(t_1) | \hat{A}_{\text{phys}}(t_1) | \text{vac}_{t_0}(t_1) \rangle \end{aligned} \quad (16)$$

More details of this approach to fermionic QFT are given in [13, 14].

3. SPATIALLY UNIFORM ELECTRIC FIELDS

A spatially uniform electric field in the z -direction can be represented by $A_\mu(t) = (0, 0, 0, A(t))$, so that $\mathbf{E}(t) = (0, 0, \dot{A}(t))$ and $\mathbf{B}(t) = \mathbf{0}$. To find solutions to the Dirac equation in this background, we try separating $\psi(x)$ as

$$\psi_{\mathbf{p}}(\mathbf{x}, t) = \psi_{\mathbf{p}}(t) e^{i\mathbf{p} \cdot \mathbf{x}} \quad (17)$$

where $\mathbf{p} \cdot \mathbf{x} = \sum_{k=1}^3 p^k x^k$. Then $\psi_{\mathbf{p}}(t)$ must satisfy:

$$i \frac{d\psi_{\mathbf{p}}(t)}{dt} = m\gamma_0 \psi_{\mathbf{p}}(t) + \bar{\mathbf{p}}_\perp \psi_{\mathbf{p}}(t) + (p^3 + eA(t)) \bar{\sigma}_3 \psi_{\mathbf{p}}(t) \quad (18)$$

where $\bar{\mathbf{p}}_\perp \equiv p^1 \bar{\sigma}_1 + p^2 \bar{\sigma}_2$. By introducing a set of basis spinors $\phi_{\pm\pm}(\mathbf{p})$ satisfying:

$$\begin{aligned} \phi_{s\lambda}^\dagger(\mathbf{p}) \phi_{s'\lambda'}(\mathbf{p}) &= \delta_{ss'} \delta_{\lambda\lambda'} & \text{for all } \mathbf{p} \\ \bar{\sigma}_3 \phi_{\pm\lambda}(\mathbf{p}) &= \pm \phi_{\pm\lambda}(\mathbf{p}) & \text{for } \lambda = \pm \text{ and all } \mathbf{p} \\ \gamma_0 \phi_{\pm\lambda}(\mathbf{p}) &= \phi_{\mp\lambda}(\mathbf{p}) & \text{for } \lambda = \pm \text{ and all } \mathbf{p} \\ \bar{\mathbf{p}}_\perp \phi_{s\lambda}(\mathbf{p}) &= s\lambda |\mathbf{p}_\perp| \phi_{-s-\lambda}(\mathbf{p}) & \text{for } s = \pm, \lambda = \pm, \text{ and all } \mathbf{p} \end{aligned}$$

where $|\mathbf{p}_\perp|^2 \equiv (p^1)^2 + (p^2)^2$, we can expand $\psi_{\mathbf{p}}(t)$ as:

$$\psi_{\mathbf{p}}(t) = \sum_{\lambda} \{ \phi_{+\lambda}(\mathbf{p}) f_{\lambda}(t) + \phi_{-\lambda}(\mathbf{p}) g_{\lambda}(t) \} \quad (19)$$

The inner product of two solutions $\psi_{\mathbf{p}}^1(\mathbf{x}, t), \psi_{\mathbf{q}}^2(\mathbf{x}, t)$ expanded as in (17) and (19) is given by:

$$\langle \psi_{\mathbf{p}}^1(\mathbf{x}, t) | \psi_{\mathbf{q}}^2(\mathbf{x}, t) \rangle = (2\pi)^3 \delta(\mathbf{p} - \mathbf{q}) \sum_{\lambda} (\bar{f}_{\lambda}^1(t) f_{\lambda}^2(t) + \bar{g}_{\lambda}^1(t) g_{\lambda}^2(t)) \quad (20)$$

Substitution of (19) into (18) gives:

$$\begin{aligned} i \frac{df_{\pm}}{dt} - (p^3 + eA(t)) f_{\pm} &= m g_{\pm} \pm |\mathbf{p}_\perp| g_{\mp} \\ i \frac{dg_{\pm}}{dt} + (p^3 + eA(t)) g_{\pm} &= m f_{\pm} \mp |\mathbf{p}_\perp| f_{\mp} \end{aligned} \quad (21)$$

Define now the dimensionless quantities

$$\tau \equiv mt \quad p_z \equiv \frac{p^3}{m} \quad p \equiv \frac{|\mathbf{p}_\perp|}{m} \quad \text{and} \quad a(\tau) = \frac{eA}{m} \quad (22)$$

This means we are measuring distances in multiples of the Compton wavelength $\frac{\lambda_c}{2\pi} = \frac{\hbar}{mc} \approx 3.9 \times 10^{-13}$ metres, and times in multiples of $\frac{\lambda_c}{2\pi c} \approx 1.3 \times 10^{-21}$ seconds (where we have used the mass and charge of the electron). Equations (21) become:

$$\begin{aligned} \left(i \frac{d}{d\tau} - (p_z + a(\tau)) \right) f_{\pm}(\tau) &= g_{\pm}(\tau) \pm p g_{\mp}(\tau) \\ \left(i \frac{d}{d\tau} + (p_z + a(\tau)) \right) g_{\pm}(\tau) &= f_{\pm}(\tau) \mp p f_{\mp}(\tau) \end{aligned} \quad (23)$$

from which we find that

$$\frac{d^2 f_{\lambda}}{d\tau^2} + \left(1 + p^2 + (p_z + a(\tau))^2 + i \frac{da}{d\tau} \right) f_{\lambda} = 0 \quad (24)$$

$$\frac{d^2 g_{\lambda}}{d\tau^2} + \left(1 + p^2 + (p_z + a(\tau))^2 - i \frac{da}{d\tau} \right) g_{\lambda} = 0 \quad (25)$$

for both λ . To construct a complete set of solutions to (18), let $f(\tau)$ be any solution of (24). One solution of (18) can then be found by putting

$f_-(\tau) = 0$, $f_+(\tau) = f(\tau)$ and using (23) to get:

$$g_+(\tau) = \frac{1}{1+p^2}h(\tau) \quad \text{and} \quad g_-(\tau) = \frac{p}{1+p^2}h(\tau) \quad (26)$$

where $h(\tau) \equiv (i\frac{d}{d\tau} - (p_z + a(\tau)))f(\tau)$. From this we obtain

$$\psi'_{\mathbf{p},1}(\mathbf{x},t) = C \left[\phi_{++}(\mathbf{p})\sqrt{1+p^2}f(\tau) + \frac{\phi_{-+}(\mathbf{p}) + p\phi_{--}(\mathbf{p})}{\sqrt{1+p^2}}h(\tau) \right] e^{i\mathbf{p}\cdot\mathbf{x}} \quad (27)$$

where $C \equiv ((1+p^2)|f|^2 + |h|^2)^{-\frac{1}{2}}$ is constant by virtue of conservation of the norm. Similarly, $\psi'_{\mathbf{p},2}(\mathbf{x},t)$ can be found by putting $f_+(\tau) = 0$ and $f_-(\tau) = f(\tau)$, and then using (23) to give $g_+(\tau)$ and $g_-(\tau)$ (in terms of $h(\tau)$). $\psi_{\mathbf{p},3}(\mathbf{x},t)$ is found by putting $g_-(\tau) = 0$, $g_+(\tau) = \bar{f}(\tau)$ (which solves equation (25)) and then using equations (23) to specify $f_{\pm}(\tau)$ in terms of $\bar{h}(\tau)$, while $\psi_{\mathbf{p},4}(\mathbf{x},t)$ is similarly found by putting $g_+(\tau) = 0$, $g_-(\tau) = \bar{f}(\tau)$. This finally allows us to generate the complete set of solutions:

$$\begin{aligned} \psi_{\mathbf{p},1}(\mathbf{x},t) &= \frac{1}{\sqrt{1+p^2}}(\psi'_{\mathbf{p},1}(\mathbf{x},t) - p\psi'_{\mathbf{p},2}(\mathbf{x},t)) \\ &= C[(\phi_{++}(\mathbf{p}) - p\phi_{+-}(\mathbf{p}))f(\tau) + \phi_{-+}(\mathbf{p})h(\tau)]e^{i\mathbf{p}\cdot\mathbf{x}} \\ \psi_{\mathbf{p},2}(\mathbf{x},t) &= \frac{1}{\sqrt{1+p^2}}(p\psi'_{\mathbf{p},1}(\mathbf{x},t) + \psi'_{\mathbf{p},2}(\mathbf{x},t)) \\ &= C[(p\phi_{++}(\mathbf{p}) + \phi_{+-}(\mathbf{p}))f(\tau) + \phi_{--}(\mathbf{p})h(\tau)]e^{i\mathbf{p}\cdot\mathbf{x}} \quad (28) \\ \psi_{\mathbf{p},3}(\mathbf{x},t) &= C \left[\frac{(-\phi_{++}(\mathbf{p}) + p\phi_{+-}(\mathbf{p}))}{\sqrt{1+p^2}}\bar{h}(\tau) + \phi_{-+}(\mathbf{p})\sqrt{1+p^2}\bar{f}(\tau) \right] e^{i\mathbf{p}\cdot\mathbf{x}} \\ \psi_{\mathbf{p},4}(\mathbf{x},t) &= C \left[\frac{(-p\phi_{++}(\mathbf{p}) - \phi_{+-}(\mathbf{p}))}{\sqrt{1+p^2}}\bar{h}(\tau) + \phi_{--}(\mathbf{p})\sqrt{1+p^2}\bar{f}(\tau) \right] e^{i\mathbf{p}\cdot\mathbf{x}} \end{aligned}$$

It is easy to verify that these solutions are mutually orthogonal and are each normalised to $(2\pi)^3\delta(\mathbf{0})$. The choice of $\psi_{\mathbf{p},1}$ and $\psi_{\mathbf{p},2}$ here (in terms of $\psi'_{\mathbf{p},1}$ and $\psi'_{\mathbf{p},2}$) is for later convenience.

3.1. Energy Eigenstates

We now calculate $\mathcal{H}^{\pm}(t_0)$ at each time t_0 . We must first decompose the space of spinor-valued functions $\psi(\mathbf{x},t_0)$ (of space, at time t_0) in terms of the spectrum of the operator $\hat{H}(t_0)$ given by:

$$\hat{H}(t_0) : \psi(\mathbf{x}, t_0) \rightarrow -i \sum_k \bar{\sigma}_k \partial_k \psi(\mathbf{x}, t_0) + eA(t_0) \bar{\sigma}_3 \psi(\mathbf{x}, t_0) + m\gamma_0 \psi(\mathbf{x}, t_0) \quad (29)$$

Consider the action of $\hat{H}(t_0)$ on plane wave states of the form (17). It is easy to see that:

$$\begin{aligned} \hat{H}(t_0) \psi_{\mathbf{p}}(\mathbf{x}, t_0) &= E_{\mathbf{p}, t_0} \psi_{\mathbf{p}}(\mathbf{x}, t_0) \text{ if and only if} \\ m\gamma_0 \psi_{\mathbf{p}}(t_0) + \bar{\mathbf{p}}_{\perp} \psi_{\mathbf{p}}(t_0) + (p^3 + eA(t_0)) \bar{\sigma}_3 \psi_{\mathbf{p}}(t_0) &= E_{\mathbf{p}, t_0} \psi_{\mathbf{p}}(t_0) \end{aligned} \quad (30)$$

By substituting $\psi_{\mathbf{p}, t_0} = \sum_{\lambda} \{\phi_{+\lambda}(\mathbf{p}) f_{\lambda, t_0} + \phi_{-\lambda}(\mathbf{p}) g_{\lambda, t_0}\}$ and using (22) we transform this into the eigenvalue problem:

$$\begin{aligned} m \begin{bmatrix} p_z + a(\tau_0) & 0 & 1 & p \\ 0 & p_z + a(\tau_0) & -p & 1 \\ 1 & -p & -p_z - a(\tau_0) & 0 \\ p & 1 & 0 & -p_z - a(\tau_0) \end{bmatrix} \begin{bmatrix} f_{+, t_0} \\ f_{-, t_0} \\ g_{+, t_0} \\ g_{-, t_0} \end{bmatrix} \\ = E_{\mathbf{p}, t_0} \begin{bmatrix} f_{+, t_0} \\ f_{-, t_0} \\ g_{+, t_0} \\ g_{-, t_0} \end{bmatrix} \end{aligned} \quad (31)$$

This matrix squares to $(m^2 + |\mathbf{p}_{\perp}|^2 + (p^3 + eEA(t_0))^2) I_4$. Its eigenvalues are therefore $E_{\mathbf{p}, t_0} = \pm \sqrt{m^2 + |\mathbf{p}_{\perp}|^2 + (p^3 + eEA(t_0))^2} = \pm mE_{\tau_0}$ in terms of the dimensionless quantity $E_{\tau} \equiv \sqrt{1 + p^2 + (p_z + a(\tau))^2}$. We consider the following cases:

Case 1: $E_{\mathbf{p}, t_0} = mE_{\tau_0}$

We seek two independent solutions of (31) with $E_{\mathbf{p}, t_0} = mE_{\tau_0}$. So that these are similar to the $\psi_{\mathbf{p}, i}(\mathbf{x}, t)$, we choose $u_{\mathbf{p}, 1, t_0}(\mathbf{x})$ such that $g_{+, t_0} = 1$ and $g_{-, t_0} = 0$. In (31) this gives:

$$u_{\mathbf{p}, 1, t_0}(\mathbf{x}) = D \frac{\phi_{++}(\mathbf{p}) - p\phi_{+-}(\mathbf{p}) + (E_{\tau_0} - p_z - a(\tau_0))\phi_{-+}(\mathbf{p})}{E_{\tau_0} - p_z - a(\tau_0)} e^{i\mathbf{p} \cdot \mathbf{x}} \quad (32)$$

where $D = \text{constant}$, and we have used the identity $(E_{\tau_0} - p_z - a(\tau_0))(E_{\tau_0} + p_z + a(\tau_0)) = 1 + p^2$. By requiring $u_{\mathbf{p}, 1, t_0}(\mathbf{x})$ to have norm $(2\pi)^3 \delta(\mathbf{0})$ we obtain $D = \sqrt{\frac{E_{\tau_0} - p_z - a(\tau_0)}{2E_{\tau_0}}}$.

Similarly, $u_{\mathbf{p},2,t_0}(\mathbf{x})$ can be found by putting $g_{+,t_0}=0$, $g_{-,t_0}=1$, and then normalising to $(2\pi)^3\delta(\mathbf{0})$. This gives:

$$u_{\mathbf{p},1,t_0}(\mathbf{x}) = \frac{\phi_{++}(\mathbf{p}) - p\phi_{+-}(\mathbf{p}) + (E_{\tau_0} - p_z - a(\tau_0))\phi_{-+}(\mathbf{p})}{\sqrt{2E_{\tau_0}(E_{\tau_0} - p_z - a(\tau_0))}} e^{i\mathbf{p}\cdot\mathbf{x}} \quad (33)$$

$$u_{\mathbf{p},2,t_0}(\mathbf{x}) = \frac{p\phi_{++}(\mathbf{p}) + \phi_{+-}(\mathbf{p}) + (E_{\tau_0} - p_z - a(\tau_0))\phi_{--}(\mathbf{p})}{\sqrt{2E_{\tau_0}(E_{\tau_0} - p_z - a(\tau_0))}} e^{i\mathbf{p}\cdot\mathbf{x}} \quad (34)$$

Case 2: $E_{\mathbf{p},t_0} = -mE_{\tau_0}$

A similar procedure gives:

$$v_{\mathbf{p},1,t_0}(\mathbf{x}) = \frac{-\phi_{++}(\mathbf{p}) + p\phi_{+-}(\mathbf{p}) + (E_{\tau_0} + p_z + a(\tau_0))\phi_{-+}(\mathbf{p})}{\sqrt{2E_{\tau_0}(E_{\tau_0} + p_z + a(\tau_0))}} e^{i\mathbf{p}\cdot\mathbf{x}} \quad (35)$$

$$v_{\mathbf{p},2,t_0}(\mathbf{x}) = \frac{-p\phi_{++}(\mathbf{p}) - \phi_{+-}(\mathbf{p}) + (E_{\tau_0} + p_z + a(\tau_0))\phi_{--}(\mathbf{p})}{\sqrt{2E_{\tau_0}(E_{\tau_0} + p_z + a(\tau_0))}} e^{i\mathbf{p}\cdot\mathbf{x}} \quad (36)$$

These states are eigenstates of the gauge invariant 3-momentum operator $-i\partial_k + eA_k$ of momentum $\mathbf{p}' = (p^1, p^2, p^3 + eA(t_0))$. Hence the 1-electron state $|(\mathbf{p}, \lambda)_{t_0}\rangle \equiv u_{\mathbf{p},\lambda,t_0} \wedge |\text{vac}_{t_0}\rangle$ has physical (gauge invariant) momentum \mathbf{p}' . The 1-positron state $|(\mathbf{p}, \lambda)_{t_0}\rangle \equiv i v_{\mathbf{p},\lambda,t_0} \wedge |\text{vac}_{t_0}\rangle$ (where $i v_{\mathbf{p},\lambda,t_0}$ removes the $v_{\mathbf{p},\lambda,t_0}$ degree of freedom from $|\text{vac}_{t_0}\rangle$ [13, 14]) has physical momentum $-\mathbf{p}'$.

Suppose now that $A(t_0) \rightarrow \mp\infty$ as $t_0 \rightarrow \pm\infty$. This holds for the constant electric field $A(t) = Et$ ($E < 0$) and many other electric fields. In this case we have:

$$\begin{aligned} \bar{\sigma}_3 u_{\mathbf{p},\lambda,-\infty}(\mathbf{x}) &= u_{\mathbf{p},\lambda,-\infty}(\mathbf{x}) & \bar{\sigma}_3 v_{\mathbf{p},\lambda,-\infty}(\mathbf{x}) &= -v_{\mathbf{p},\lambda,-\infty}(\mathbf{x}) \\ \bar{\sigma}_3 u_{\mathbf{p},\lambda,\infty}(\mathbf{x}) &= -u_{\mathbf{p},\lambda,\infty}(\mathbf{x}) & \bar{\sigma}_3 v_{\mathbf{p},\lambda,\infty}(\mathbf{x}) &= v_{\mathbf{p},\lambda,\infty}(\mathbf{x}) \end{aligned}$$

It follows that any electron (of charge $e < 0$) in this electric field, that has a finite momentum at finite time, will at late times be moving in the negative x^3 direction with infinite momentum (i.e. at speeds approaching that of light), whereas a positron with charge $-e$ will be moving in the positive x^3 direction with infinite momentum. At very early times this situation is reversed. Clearly it is important to keep track of what constitutes particles/antiparticles at different times, since not only does this change with time in an electric field, but here the spaces \mathcal{H}^\pm have completely reversed between early and late times; $\mathcal{H}^\pm(-\infty) = \mathcal{H}^\mp(\infty)$! This fact is also mentioned in [7].

3.2. Finite Time Transition Probabilities

We now have the positive/negative energy eigenstates $\{|u_{\mathbf{p},\lambda;t_0}\rangle, |v_{\mathbf{p},\lambda;t_0}\rangle\}$ at each time t_0 , and the evolution operator:

$$\hat{U}_1(t_1, t_0) = \int \frac{d^3\mathbf{p}'}{(2\pi)^3} \sum_{i=1}^4 |\psi_{\mathbf{p}',i}(t_1)\rangle \langle \psi_{\mathbf{p}',i}(t_0)|$$

Hence we can write $|u_{\mathbf{p},\lambda;t_0}(t_1)\rangle = \hat{U}_1(t_1, t_0)|u_{\mathbf{p},\lambda;t_0}\rangle$, $|v_{\mathbf{p},\lambda;t_0}(t_1)\rangle = \hat{U}_1(t_1, t_0)|v_{\mathbf{p},\lambda;t_0}\rangle$ and the time-dependent Bogoliubov coefficients become

$$\begin{aligned} S_{\mathbf{p},\lambda;\mathbf{q},\sigma}(t_1, t_0) &= \begin{bmatrix} \alpha_{\mathbf{p},\lambda;\mathbf{q},\sigma}(t_1, t_0) & \beta_{\mathbf{p},\lambda;\mathbf{q},\sigma}(t_1, t_0) \\ \gamma_{\mathbf{p},\lambda;\mathbf{q},\sigma}(t_1, t_0) & \epsilon_{\mathbf{p},\lambda;\mathbf{q},\sigma}(t_1, t_0) \end{bmatrix} \\ &= \begin{bmatrix} \langle u_{\mathbf{p},\lambda;t_1}(\mathbf{x}) | \hat{U}_1(t_1, t_0) | u_{\mathbf{q},\sigma;t_0}(\mathbf{x}) \rangle & \langle u_{\mathbf{p},\lambda;t_1}(\mathbf{x}) | \hat{U}_1(t_1, t_0) | v_{\mathbf{q},\sigma;t_0}(\mathbf{x}) \rangle \\ \langle v_{\mathbf{p},\lambda;t_1}(\mathbf{x}) | \hat{U}_1(t_1, t_0) | u_{\mathbf{q},\sigma;t_0}(\mathbf{x}) \rangle & \langle v_{\mathbf{p},\lambda;t_1}(\mathbf{x}) | \hat{U}_1(t_1, t_0) | v_{\mathbf{q},\sigma;t_0}(\mathbf{x}) \rangle \end{bmatrix} \\ &= \int \frac{d^3\mathbf{p}'}{(2\pi)^3} \sum_{i=1}^4 M_{\mathbf{p},\lambda;\mathbf{p}',i}(\tau_1) \bar{M}_{\mathbf{q},\sigma;\mathbf{p}',i}(\tau_0) \end{aligned} \quad (37)$$

where:

$$M_{\mathbf{p},\lambda;\mathbf{p}',i}(\tau) = \begin{bmatrix} \langle u_{\mathbf{p},\lambda;t}(\mathbf{x}) | \psi_{\mathbf{p}',i}(\mathbf{x}, t) \rangle \\ \langle v_{\mathbf{p},\lambda;t}(\mathbf{x}) | \psi_{\mathbf{p}',i}(\mathbf{x}, t) \rangle \end{bmatrix} \quad (38)$$

which is unitary for all time, since it describes the overlap between two orthonormal sets of states.

We can now use (33) - (36) and (28) to calculate $\mathbf{M}(\tau)$ as

$$M_{\mathbf{p},\lambda;\mathbf{p}',i}(\tau) = (2\pi)^3 \delta(\mathbf{p} - \mathbf{p}') \begin{bmatrix} A_{p,p_z}(\tau) I_2 & -\bar{B}_{p,p_z}(\tau) I_2 \\ B_{p,p_z}(\tau) I_2 & \bar{A}_{p,p_z}(\tau) I_2 \end{bmatrix} \quad (39)$$

where

$$A_{p,p_z}(\tau) = \frac{C}{\sqrt{2E_\tau(E_\tau - p_z - a(\tau))}} ((E_\tau - p_z - a(\tau))h(\tau) + (1 + p^2)f(\tau)) \quad (40)$$

$$= C \sqrt{\frac{E_\tau - p_z - a(\tau)}{2E_\tau}} \left(i \frac{df}{d\tau} + E_\tau f \right) \quad (41)$$

$$B_{p,p_z}(\tau) = \frac{C}{\sqrt{2E_\tau(E_\tau + p_z + a(\tau))}} ((E_\tau + p_z + a(\tau))h(\tau) - (1 + p^2)f(\tau)) \quad (42)$$

$$= C \sqrt{\frac{E_\tau + p_z + a(\tau)}{2E_\tau}} \left(i \frac{df}{d\tau} - E_\tau f \right) \quad (43)$$

and I_2 is the 2×2 identity matrix. From (39) we have

$$S_{\mathbf{p},\lambda;\mathbf{q},\sigma}(\tau_1, \tau_0) = (2\pi)^3 \delta(\mathbf{p} - \mathbf{q}) \begin{bmatrix} \alpha_{p,p_z}(\tau_1, \tau_0) I_2 & \beta_{p,p_z}(\tau_1, \tau_0) I_2 \\ -\beta_{p,p_z}(\tau_1, \tau_0) I_2 & \bar{\alpha}_{p,p_z}(\tau_1, \tau_0) I_2 \end{bmatrix} \quad (44)$$

where:

$$\alpha_{p,p_z}(\tau_1, \tau_0) \equiv A_{p,p_z}(\tau_1) \bar{A}_{p,p_z}(\tau_0) + \bar{B}_{p,p_z}(\tau_1) B_{p,p_z}(\tau_0) \quad (45)$$

$$\beta_{p,p_z}(\tau_1, \tau_0) \equiv A_{p,p_z}(\tau_1) \bar{B}_{p,p_z}(\tau_0) - \bar{B}_{p,p_z}(\tau_1) A_{p,p_z}(\tau_0) \quad (46)$$

We can now use the formulae in Section 2.3 to extract from (44) whatever information we wish about this system of electrons evolving in a background $\mathbf{E} = (0, 0, \dot{A}(t))$, expressed in terms of an arbitrary solution to equation (24). For example, suppose we start the system at some initial time t_0 in the vacuum state $|\text{vac}_{t_0}\rangle$, and let this state evolve until some later time t_1 . Then, from (15), the expected number of particles per unit volume in this evolved vacuum (not including antiparticles) with spin λ and physical (gauge-invariant) 3-momentum $\mathbf{p}' = (p^1, p^2, p^3 + eA(t_1))$ in a range $d^3\mathbf{p}$ about \mathbf{p}' is given by:

$$\frac{N_{\mathbf{p},\lambda,t_0}(t_1) d^3\mathbf{p}}{V} = |\beta_{p,p_z}(\tau_1, \tau_0)|^2 d^3\mathbf{p} \quad (47)$$

(where $V = (2\pi)^3 \delta(\mathbf{0})$). The the same number of antiparticles is also created with physical momenta $-\mathbf{p}'$. The total number of particles per unit volume

in this evolved vacuum (including antiparticles) is therefore

$$\begin{aligned} \frac{N_{\text{vac},t_0}(t_1)}{V} &= 2 \sum_{\lambda} \int \frac{d^3 \mathbf{p}}{(2\pi)^3} |\beta_{p,p_z}(\tau_1, \tau_0)|^2 \\ &= \frac{m^3}{\pi^2} \int_{-\infty}^{\infty} dp_z \int_0^{\infty} dp p |\beta_{p,p_z}(\tau_1, \tau_0)|^2 \end{aligned} \quad (48)$$

The probability that this state is vacuum at time t_1 is determined from (5), using $\det(e^A) = e^{\text{Trace}(A)}$, to give

$$\mathcal{P}_{|\text{vac}_{t_0}\rangle \rightarrow |\text{vac}_{t_1}\rangle} = \exp \left(\frac{m^3 V}{2\pi^2} \int_{-\infty}^{\infty} dp_z \int_0^{\infty} dp p \log(1 - |\beta_{p,p_z}(\tau_1, \tau_0)|^2) \right) \quad (49)$$

From (33) - (36), the total current density in this evolved vacuum is (13) and $\hat{J}_{1,k} = e\bar{\sigma}_k$)

$$\begin{aligned} \frac{J_{\text{vac},3,t_0}(t_1)}{V} &= \frac{em^3}{\pi^2} \int_{-\infty}^{\infty} dp_z \int_0^{\infty} \frac{dp p}{E_{\tau_1}} \{ (p_z + a(\tau_1)) |\beta_{p,p_z}(\tau_1, \tau_0)|^2 \\ &\quad - \sqrt{1+p^2} \Re(\beta_{p,p_z}(\tau_1, \tau_0) \alpha_{p,p_z}(\tau_1, \tau_0)) \} \end{aligned} \quad (50)$$

where $J_{\text{vac},1,t_0}(t_1) = 0 = J_{\text{vac},2,t_0}(t_1)$ by symmetry. This expression will generally contain a logarithmic divergence proportional to $\ddot{a}(\tau)$, which must be isolated and absorbed into a renormalisation of the coupling constant e . In Section 4, $\ddot{a}(\tau) = 0$ so that no renormalisation is necessary. For most of Section 5 we use a cut-off in the integrals such that the cut-off-dependent renormalisation term is small, and can be ignored.

Non-Vacuum Initial Conditions

Consider an initial state at time t_0 consisting of N particles having momenta $\mathbf{p}_1, \dots, \mathbf{p}_N$ and spins $\lambda_1, \dots, \lambda_N$. From equations (16) and (44), the expected number of out particles at some later time t_1 is:

$$N_{\text{out},t_0}(t_1) = \sum_{i=1}^N (|\alpha_{p_i,p_{z,i}}(\tau_1, \tau_0)|^2 - |\beta_{p_i,p_{z,i}}(\tau_1, \tau_0)|^2) + N_{\text{vac},t_0}(t_1) \quad (51)$$

which is less than $N_{\text{vac},t_0}(t_1) + N$ due to Pauli exclusion (recall that

$$|\alpha_{p,p_z}(\tau_1, \tau_0)|^2 + |\beta_{p,p_z}(\tau_1, \tau_0)|^2 = 1).$$

The probability that the out state contains exactly N particles is:

$$\mathcal{P}_{N \rightarrow N, t_0}(t_1) = \frac{\mathcal{P}_{|\text{vac}_{t_0}\rangle \rightarrow |\text{vac}_{t_1}\rangle}}{\prod_{i=1}^N |\alpha_{p_i, p_z, i}(\tau_1, \tau_0)|^2} \quad (52)$$

This expression highlights the well-known fact that particle creation is less likely in a state that already contains particles. The current density of this evolved state is:

$$J_{\text{out}, t_0}(t_1) = \sum_{i=1}^N J(u_{\mathbf{p}_i, \lambda_i, t_0}(\mathbf{x}, t_1)) + J_{\text{vac}, t_0}(t_1) \quad (53)$$

where from (44)

$$u_{\mathbf{p}, \lambda, t_0}(\mathbf{x}, t_1) = \alpha_{p, p_z}(\tau_1, \tau_0) u_{\mathbf{p}, \lambda, t_1}(\mathbf{x}) - \bar{\beta}_{p, p_z}(\tau_1, \tau_0) v_{\mathbf{p}, \lambda, t_1}(\mathbf{x})$$

so that

$$\begin{aligned} J(u_{\mathbf{p}, \lambda, t_0}(\mathbf{x}, t_1)) &= \frac{e}{E_{\tau_1}} \{ (1 - 2|\beta_{p, p_z}(\tau_1, \tau_0)|^2)(p_z + a(\tau_1)) \\ &\quad + 2\sqrt{1 + p^2} \Re(\alpha_{p, p_z}(\tau_1, \tau_0)\beta_{p, p_z}(\tau_1, \tau_0)) \} \quad (54) \end{aligned}$$

Simplification

Although $\mathbf{M}(t)$ depends on the initial conditions chosen for $f(\tau)$ in (24), the elements of $\mathbf{S}(t_1, t_0)$ do not depend on them. We can, however, by an appropriate choice of initial conditions, simplify the expression for $\mathbf{S}(t_1, t_0)$. Impose temporarily the conditions $f(\tau_0) = 1$ and $h(\tau_0) = E_{\tau_0} - p_z - a(\tau_0)$. (This second condition is equivalent $i \frac{df}{d\tau} \big|_{\tau=\tau_0} = E_{\tau_0} f(\tau_0)$, revealing a connection between our particle definition and that motivated by ‘instantaneous frequency’.) These conditions yield $A_{p,p_z}(\tau_0) = 1$ and $B_{p,p_z}(\tau_0) = 0$. Hence we can identify $\psi_{\mathbf{p},i}(t) = u_{\mathbf{p},i,t_0}(t)$ and $\psi_{\mathbf{p},i+2}(t) = v_{\mathbf{p},i,t_0}(t)$ for $i = 1, 2$, so that $\alpha_{p,p_z}(\tau_1, \tau_0) = A_{p,p_z}(\tau_1)$ and $\beta_{p,p_z}(\tau_1, \tau_0) = -\bar{B}_{p,p_z}(\tau_1)$ in this case. The current density in the evolved vacuum then simplifies to:

$$J_{\text{vac},3,t_0}(t_1) = \frac{em^3}{2\pi^2} \int_{-\infty}^{\infty} dp_z \int_0^{\infty} dp \, p \left\{ \frac{E_{\tau_1} + p_z + a(\tau_1)}{E_{\tau_1}} - \frac{E_{\tau_0} + p_z + a(\tau_0)}{E_{\tau_0}} |f(\tau_1)|^2 \right\} \quad (55)$$

and $J(u_{\mathbf{p}_i, \lambda_i, t_0}(\mathbf{x}, t_1))$ becomes:

$$J(u_{\mathbf{p}_i, \lambda_i, t_0}(\mathbf{x}, t_1)) = e \left\{ \frac{E_{\tau_0} + p_z + a(\tau_0)}{E_{\tau_0}} |f(\tau_1)|^2 - 1 \right\} \quad (56)$$

These simplifications will be used in Section 5.

4. CONSTANT ELECTRIC FIELD

For constant electric field we have $a(\tau) = \frac{eE}{m^2} \tau \equiv a_0 \tau$. Since e is negative, positive a_0 corresponds to an electric field in the $-z$ direction. By writing $a_0 = -\frac{E}{E_c}$ we identify the ‘natural’ electric field strength $E_c = \frac{m^2 c^3}{|e| \hbar} \approx 1.3 \times 10^{18} \text{ V m}^{-1}$ (where we have substituted the mass and absolute charge of the electron). This corresponds to an electromagnetic energy density of approximately 137 electron rest mass energies per Compton volume $\left(\frac{\hbar}{mc}\right)^3$, and is too large to be produced on macroscopic scales in the laboratory, although astrophysical examples have been considered [24, 25]. Also, fields of this strength would be present on a microscopic scale in superheavy nuclei with charges greater than $137|e|$.

Equation (24) can now be written as:

$$\frac{d^2 f}{d\tau^2} + (1 + p^2 + (p_z + a_0 \tau)^2 + i a_0) f = 0 \quad (57)$$

Comparison with equation 8.2(1) of [26] reveals that solutions of this equation are linear combinations of $D_{\nu_p-1}(\pm \frac{1-i}{\sqrt{a_0}}(p_z+a_0\tau))$ and $D_{-\nu_p}(\pm \frac{1+i}{\sqrt{a_0}}(p_z+a_0\tau))$, where $\nu_p \equiv \frac{i(1+p^2)}{2a_0}$ and $D_\nu(z)$ are parabolic cylinder functions. We choose $f(\tau) \equiv D_{\nu_p-1}(\frac{i-1}{\sqrt{a_0}}(p_z+a_0\tau))$, which gives (after exploiting properties of the parabolic cylinder functions)

$$h(\tau) = (1+i)D_{\nu_p}\left(\frac{i-1}{\sqrt{a_0}}(p_z+a_0\tau)\right) \text{ and } C = \frac{e^{-\frac{\pi(1+p^2)}{8a_0}}}{\sqrt{2}}$$

The first point about these expressions is that $f(\tau)$ (and hence $A_{p,p_z}(\tau)$ and $B_{p,p_z}(\tau)$) depends only on p_z and τ through the combination $p_z+a_0\tau$, which is the physical z -momentum (in units of mass) at time τ of the state labelled by the subscript \mathbf{p} . This allows us to write $A_{p,p_z}(\tau_1) = A_{p,p_z^{\text{out}}}(0)$ where $p_z^{\text{out}} \equiv p_z+a_0\tau_1$, so that the evolution matrix can be written as:

$$S_{\mathbf{p},\lambda;\mathbf{q},\sigma}(\tau_1,\tau_0) = (2\pi)^3 \delta(\mathbf{p}-\mathbf{q}) \begin{bmatrix} \alpha_{p,p_z^{\text{out}}}(0,-\tau)I_2 & \beta_{p,p_z^{\text{out}}}(0,-\tau)I_2 \\ -\beta_{p,p_z^{\text{out}}}(0,-\tau)I_2 & \bar{\alpha}_{p,p_z^{\text{out}}}(0,-\tau)I_2 \end{bmatrix}$$

and depends only on the evolution time $\tau \equiv \tau_1 - \tau_0$. This follows from the time-translation invariance of the constant electric field.

We now recognise that the physically relevant infinite-time scattering matrix is:

$$\lim_{\tau \rightarrow \infty} S_{\mathbf{p},\lambda;\mathbf{q},\sigma}(0,-\tau) = (2\pi)^3 \delta(\mathbf{p}-\mathbf{q}) \begin{bmatrix} A_{p,p_z^{\text{out}}}(0)I_2 & -\bar{B}_{p,p_z^{\text{out}}}(0)I_2 \\ B_{p,p_z^{\text{out}}}(0)I_2 & \bar{A}_{p,p_z^{\text{out}}}(0)I_2 \end{bmatrix} \quad (58)$$

where we have used asymptotic properties of $A_{p,p_z^{\text{out}}}(\tau)$ and $B_{p,p_z^{\text{out}}}(\tau)$ and discarded unimportant phase factors. The expected number of particles per unit volume in the infinitely evolved vacuum is now

$$\frac{N_{\mathbf{p},\lambda}(\infty)}{V} = |B_{p,p_z^{\text{out}}}(0)|^2 \quad (59)$$

$$= \frac{e^{-\frac{\pi(1+p^2)}{4a_0}}}{4E_0(E_0+p_z^{\text{out}})} \left| (E_0+p_z^{\text{out}})(1+i)D_{\frac{i(1+p^2)}{2a_0}}\left(\frac{i-1}{\sqrt{a_0}}p_z^{\text{out}}\right) - (1+p^2)D_{\frac{i(1+p^2)}{2a_0}-1}\left(\frac{i-1}{\sqrt{a_0}}p_z^{\text{out}}\right) \right|^2 \quad (60)$$

Curves of this expression for various values of a_0 are shown in Figure 1. We see that $N_{\mathbf{p},\lambda}(\infty)$ is effectively zero for negative p_z^{out} , and approaches $e^{-\frac{\pi(1+p^2)}{a_0}}$ for large p_z^{out} . in agreement with [11]. The result is plausible since

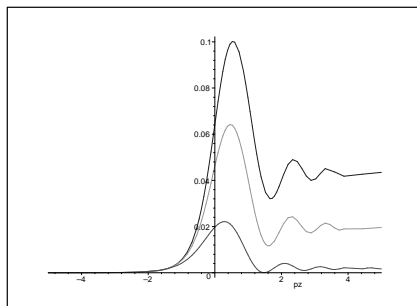


FIG. 1(A). Number density in an infinitely evolved vacuum as a function of p_z^{out} , for $a_0 = 1$ and $p = 0$ (top curve), 0.5 (middle curve), and 1 (bottom curve).

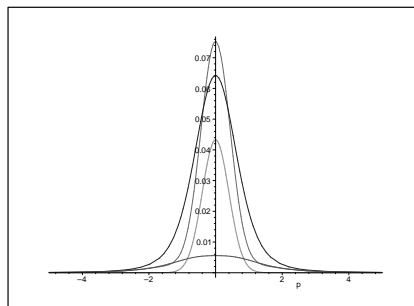


FIG. 1(B). Number density in an infinitely evolved vacuum as a function of p for $a_0 = 1$ and $p_z^{\text{out}} = -1$ (bottom curve), 0 (outermost curve), 1 (top curve) and 5 (innermost curve). A plot of $e^{-\frac{\pi(1+p^2)}{a_0}}$ is also included, which coincides almost exactly with the curve for $p_z^{\text{out}} = 5$.

any particle, once created, will be accelerated to ever increasing p_z^{out} by the electric field. The number density of created antiparticles is identical, but with the sign of p_z^{out} reversed.

A common misconception is that $\frac{N_{\mathbf{p},\lambda}(\infty)}{V} = e^{-\frac{\pi(1+p^2)}{a_0}}$ independent of p_z^{out} [2]. This misconception stems from taking $\tau_1 \rightarrow \infty$ and $\tau_0 \rightarrow -\infty$ when defining ‘in’ and ‘out’ modes, inadvertently taking the limit as $p_z^{\text{out}} \rightarrow \infty$. A more relevant result, which allows Schwinger’s formula to be derived in the large time limit, is described below.

Figure 2 shows the expected number density $N_{\mathbf{p},\lambda}(\tau)$ in the evolved vacuum for $a_0 = 1$ and $p = 1$, as a function of p_z^{out} , after an evolution time $\tau = 7$ (right), 4, 2 and 0.5 (single peak). A graph for $\tau = \infty$ is also included, which is seen to fit the left peak of the $\tau = 7$ line, and becomes constant at large p_z^{out} . The finite time behaviour demonstrated here agrees with that presented in [6]. Figure 2 has an interesting physical interpretation. At early times, particles are created mainly with p_z^{out} close to zero (Figure 1(B) shows that small p is also favoured), as expected, since these pairs require the least creation energy. At later times, the right peak represents the same early-time particles (which have been accelerated by the electric field), and the left peak represents recently created pairs, again at low momenta. Figure 3(A) shows $\frac{N_{\text{vac}}(\tau)}{Vm^3}$ for $a_0 = \frac{1}{2}$, 1 and 2.

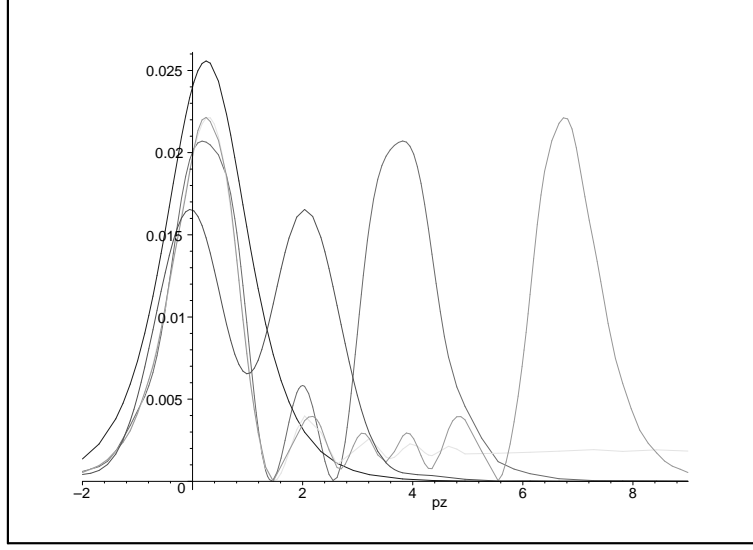


FIG. 2. Number density in the evolved vacuum, as a function of p_z^{out} , for $a_0 = 1$, $p = 1$, and $\tau = 7$ (right), 4, 2 and 0.5 (single peak). A graph for $\tau = \infty$ is included, which is seen to fit the left peak of the $\tau = 7$ line and becomes constant at large p_z^{out} .

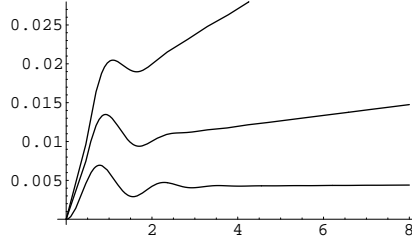


FIG. 3(A). Total number of particles in a Compton volume m^{-3} of the evolved vacuum as a function of τ for $a_0 = \frac{1}{2}$ (bottom curve), 1 and 2 (top curve).

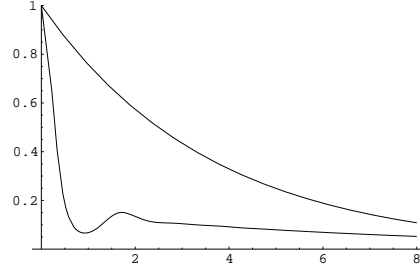


FIG. 3(B). Vacuum-vacuum transition probability for $a_0 = 1$ and $V = 40\pi^2 m^{-3}$. The initial burst of pair creation reduces the exact transition probability (bottom curve) below Schwinger's prediction (top curve) at early times.

From Figure 2 we see that for large τ , $N_{\mathbf{p},\lambda}(\tau)$ can be well approximated by

$$N_{\mathbf{p},\lambda}(\tau) \approx e^{\frac{-\pi(1+p^2)}{a_0}} (\theta(p_z^{\text{out}}) - \theta(a_0\tau - p_z^{\text{out}})) \quad (61)$$

where $\theta(p_z^{\text{out}})$ is the Heavyside step function. This allows us to approximate:

$$\int N_{\mathbf{p},\lambda}(\tau) dp_z^{\text{out}} \approx a_0 \tau e^{\frac{-\pi(1+p^2)}{a_0}} \quad (62)$$

from which we obtain the total number of pairs created:

$$N_{TOT}(\tau) \approx \frac{(eE)^2 V t}{4\pi^3} e^{\frac{-\pi m^2}{|eE|}} \text{ for large } t \equiv \frac{\tau}{m} \quad (63)$$

This analysis correctly predicts the final gradient of the graphs in Figure 3(A), and is the result most commonly referred to in the literature [6, 2, 22]. However, we see in Figure 3(A) that for $|E| \ll E_c$ the dominant contribution to the total number of produced pairs comes not from this final gradient, but from the initial burst of pair creation. Even for $|E| = \frac{1}{2}E_c$, approximately 0.44 particles are created in a volume λ_c^3 in the first 10^{-20} seconds, with only ~ 0.005 particles every 10^{-20} seconds thereafter. For $|E| = \frac{E_c}{10}$ approximately 0.014 particles are created in a volume λ_c^3 in the first 2.5×10^{-20} seconds, with only 8.6×10^{-15} particles created every 2.5×10^{-20} seconds thereafter. This difference becomes exponentially more pronounced as the ratio $|\frac{E_c}{E}|$ increases.

Similarly, substitution of (61) into (49) together with the relation

$$\log(1 - e^{\frac{-\pi\lambda}{a_0}}) = - \sum_{n=1}^{\infty} \frac{e^{\frac{-\pi n\lambda}{a_0}}}{n}$$

, gives

$$\mathcal{P}_{\text{vac} \rightarrow \text{vac}}(\tau) \approx \exp \left[\frac{-(eE)^2 V t}{4\pi^3} \sum_{n=1}^{\infty} \frac{1}{n^2} e^{\frac{-\pi n m^2}{eE}} \right] \text{ for } \tau \text{ large.} \quad (64)$$

in agreement with Schwinger's original calculation [1] (also in [27], [2], [6]). In Figure 3(B) we show the exact vacuum-vacuum transition probability, and the large time approximation of (64) for $a_0 = 1$ (we have taken $V = 40\pi^2 \text{ m}^{-3}$ for convenience).

Vacuum Current, and Induced Electric Field

Figure 4 shows the integrand in $J_{\text{vac},3,t_0}(t_1)$ from (50) as a function of p_z^{out} for various evolution times, and includes a graph of the $|\beta|^2$ contribution.

We recognise that at late times the dominant contribution to the integral comes from the $|\beta|^2$ term; the other term generates rapid oscillations

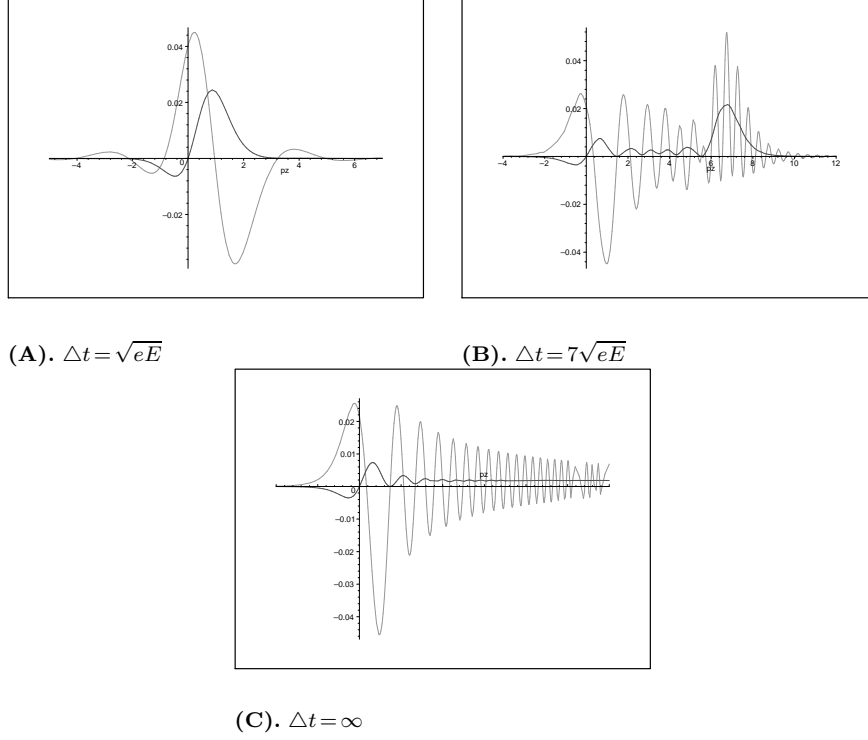


FIG. 4. Current density in an evolved vacuum after time $\Delta t = \sqrt{eE}$ (A), $7\sqrt{eE}$ (B) and ∞ (C), as a function of p_z , for $a_0 = 1$ and $p = 1$. The $|\beta|^2$ contribution is also shown (darker curve). In (B) and (C) this term provides the dominant contribution, with the $\Re(\beta\alpha)$ term producing rapid oscillations about it.

about this contribution. The $|\beta|^2$ term is the ‘classical’ contribution of the form ‘sum over created particles of the current of each particle’, while the oscillatory $\Re(\beta\alpha)$ term represents quantum interference effects. These oscillations are on a time scale $t_{qu} \sim \frac{\lambda_c}{2\pi c} = \frac{\hbar}{m}$ and a length scale of $\Delta z \sim \lambda_c$, as are the smaller, more strongly damped oscillations already present in the $|\beta|^2$ term. Oscillations on the time scale of t_{qu} can be identified with those mentioned in [11] and [28] as significant in quantum decoherence and effective dissipation processes. Figure 5 shows the total vacuum current density as a function of τ , together with the $|\beta|^2$ contribution, and the approximation that results from ignoring the $\Re(\beta\alpha)$ terms and using (61).

The $|\beta|^2$ contribution shows good agreement with Figure 5 of Kluger, Mottola et al. [11] (though they use a different scale). We also see that, although the ‘semiclassical’ $|\beta|^2$ term dominates after the first 10^{-20} seconds,

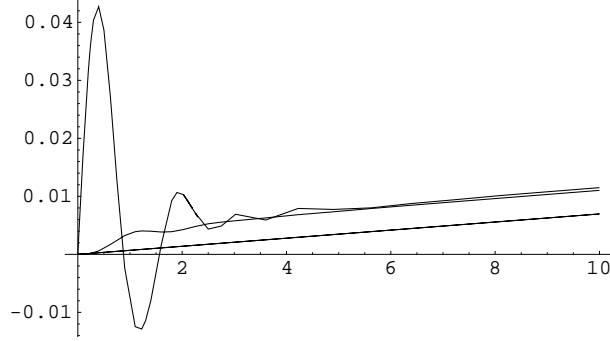


FIG. 5. Total current in a Compton volume m^{-3} of an evolved vacuum as a function of τ . The $|\beta|^2$ contribution is also shown, providing an accurate approximation except at very early times. The late time approximation of (65) is also included, which has correct final gradient but misses the initial ‘burst’ of creation, as with the total number of created particles.

the ‘quantum interference’ term is significantly more important in this first instant. Finally, although we have $J_{1,\text{vac}}(\tau) = 0 = J_{2,\text{vac}}(\tau)$ by symmetry, the integrands of $J_{1,\text{vac}}(\tau)$ and $J_{2,\text{vac}}(\tau)$ still display rapid oscillatory dependence on p_z^{out} .

The large-time approximation of $J_{3,\text{vac}}(\tau)$, obtained by ignoring the $\Re(\alpha\beta)$ term and using (61), is:

$$J_{3,\text{vac}}(\tau) \approx \frac{e(eE)^2 \Delta t}{2\pi^3} e^{-\frac{\pi m^2}{eE}} \quad (65)$$

This would generate an induced electric field in the positive z-direction:

$$E_{\text{ind}}(\tau) \approx \frac{e(eE)^2 (\Delta t)^2}{4\pi^3} e^{-\frac{\pi m^2}{eE}} \quad (66)$$

We have not taken back-reaction into account, so these results can only be considered realistic at times when $E_{\text{ind}} \ll |E|$, implying $\Delta t \ll \sqrt{\frac{\pi}{\alpha}} \frac{e^{\frac{\pi}{2}} \frac{|E|}{E_c}}{\sqrt{eE}}$. For small electric fields (where $eE \ll m^2$) this approximation is valid for an exponentially long time. It never holds for an infinite time, however, so calculations of infinite time pair creation effects without including back-reaction have little meaning. In fact, for $|E| \sim E_c$ this approximation is valid only for $\Delta t \sim 10^{-19}$ seconds!

Non-Vacuum initial conditions

As an example of a non-vacuum initial condition, consider the state $u_{\mathbf{p}_{\text{in}}, \lambda, t_0}(t) \wedge |\text{vac}_{t_0}(t)\rangle$, which at time t_0 contained one particle with mo-

momentum \mathbf{p}_{in} . Recall from equation (54) that $J(u_{\mathbf{p}_{\text{in}},\lambda,t_0}(t))$ does not represent the current at time t of this particle. Rather, $J(u_{\mathbf{p}_{\text{in}},\lambda,t_0}(t)) + J_{\text{vac}}(\tau)$ represents the expected current at time $t_0 + \frac{\tau}{m}$ of this state, which can no longer be viewed as containing one particle. This current will contain contributions not only from the 1-particle component of the evolved state, but also from the entire evolved state. Notice that, from equation (50), $J_{\text{vac}}(\tau)$ contains a factor V , while $J(u_{\mathbf{p}_{\text{in}},1,t_0}(t))$ does not. The vacuum contribution is that of a uniform current density pervading all space, and the contribution from $J(u_{\mathbf{p}_{\text{in}},\lambda,t_0}(t))$ represents a single particle moving on this ‘sea of current’.

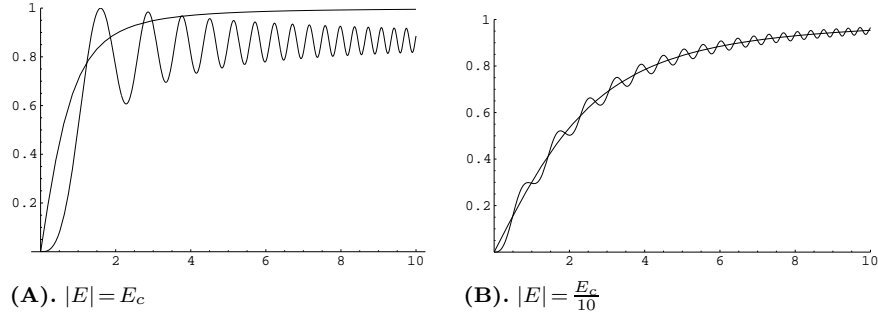


FIG. 6. $J(u_{\mathbf{p}_{\text{in}},\lambda,t_0}(\mathbf{x}, t_0 + \frac{\tau}{\sqrt{eE}}))$ as a function of τ , for $\mathbf{p}_{\text{in}} = 0$ and $|E| = E_c$ (A) and $\frac{E_c}{10}$ (B). Also included is the classically expected current for a particle accelerated from rest in this electric field. As expected, the full result is closer to the classical result in (B) than in (A).

Figure 6 shows the z -component of $J(u_{\mathbf{p}_{\text{in}},\lambda,t_0}(\mathbf{x}, t))$ as a function of τ , for $\mathbf{p}_{\text{in}} = 0$ and $|E| = E_c$ (A), and $\frac{E_c}{10}$ (B). Also included in these graphs is the classical current for a single particle accelerating from rest in the relevant electric field. For $|E| = E_c$ the classical result differs significantly from the quantum result, even when the vacuum contribution $J_{\text{vac}}(\tau)$ (from Figure 9) is included. This can be understood as follows. From equation (11) the vacuum current density is simply the sum over all modes of the difference between the two curves on these graphs (with the sign reversed, since it is negative energy modes that appear in (11)). We know from the curves in Figure 4 that this difference can be expressed as the sum of two contributions. The $\Re(\alpha\bar{\beta})$ term, which explains the ‘zitterbewegung’ oscillations in Figure 6, and the $|\beta|^2$ term, which explains the difference in height between the two graphs, and represents the probability that the particle falls into a hole in the Dirac Sea vacated by a newly freed $v_{\mathbf{p}}$ degree of freedom. This interpretation is also supported by Figures (13), (14) and

(16) of the ‘adiabatic’ case. For $|E| = \frac{E_c}{10}$, for which the probability of particle creation is small, the quantum result agrees well with the classical prediction. The graph for $|E| = \frac{E_c}{100}$ is not included since the quantum result becomes indistinguishable from the classical prediction. Finally, if at time t we project out the 1-particle component of $u_{\mathbf{p}_{\text{in}},1,t_0}(t) \wedge |\text{vac}_{t_0}(t)\rangle$ (for example if the wave-function ‘collapsed’ during a measurement of particle numbers) and measure the current of this projected state, we again obtain the classical 1-particle prediction.

5. ADIABATIC ELECTRIC FIELD

Consider now the spatially uniform electric field $E(t) = E \text{sech}^2(\frac{mt}{\rho})$. This is generated by: $a(\tau) = a_0 \rho \tanh\left(\frac{\tau}{\rho}\right)$. Hence, (24) becomes

$$\frac{d^2 f_\lambda}{d\tau^2} + \left[1 + p^2 + \left(p_z + a_0 \rho \tanh\left(\frac{\tau}{\rho}\right) \right)^2 + i a_0 \text{sech}^2\left(\frac{\tau}{\rho}\right) \right] f_\lambda = 0 \quad (67)$$

To solve this equation we use the same procedure as in [2]. Define

$$y \equiv \frac{1}{2} \left(1 + \tanh\left(\frac{\tau}{\rho}\right) \right) \\ f(\tau) = g(y(\tau)) e^{-iE_{-\infty}\tau} (1 + e^{\frac{2\tau}{\rho}})^{-\frac{i\rho\Delta E}{2}} \quad (68)$$

so that we can rewrite (67) as:

$$y(1-y) \frac{d^2 g}{dy^2} + \{1 - i\rho E_{-\infty} - (2 + i\rho\Delta E)y\} \frac{dg}{dy} - \nu_- (1 + \nu_+) g = 0 \quad (69)$$

where $\Delta E \equiv E_{+\infty} - E_{-\infty}$ is the change in energy caused by evolution from $\tau = -\infty$ to $\tau = +\infty$ in this electric field, $\Delta p_z = 2a_0\rho$ is the corresponding change in z -momentum, and we have defined $\nu_\pm \equiv \frac{i\rho}{2}(\Delta E \pm \Delta p_z)$. It follows (see [26], pg 56) that a possible solution is the hypergeometric function

$g(y) = F(\nu_-, 1 + \nu_+; 1 - i\rho E_{-\infty}; y)$, from which we find that

$$\begin{aligned}
f(\tau) &= F(\nu_-, 1 + \nu_+; 1 - i\rho E_{-\infty}; y(\tau)) e^{-iE_{-\infty}\tau} (1 + e^{\frac{2\tau}{\rho}})^{\frac{-i\rho\Delta E}{2}} \\
h(\tau) &= \left\{ \frac{2i\nu_-}{\rho} (1 - y(\tau)) F(1 + \nu_-, 1 + \nu_+; 1 - i\rho E_{-\infty}; y(\tau)) \right. \\
&\quad \left. + (E_{+\infty} - p_z - a_0\rho) F(\nu_-, 1 + \nu_+; 1 - i\rho E_{-\infty}; y(\tau)) \right\} e^{-iE_{-\infty}\tau} (1 + e^{\frac{2\tau}{\rho}})^{\frac{-i\rho\Delta E}{2}} \\
C^{-2} &= 2E_{-\infty}(E_{-\infty} - p_z + a_0\rho)
\end{aligned} \tag{70}$$

We have again made this choice of $f(\tau)$ and $h(\tau)$ so that $B_{p,p_z}(\tau) \rightarrow 0$ as $\tau \rightarrow -\infty$ and we can write $\mathcal{S}(\tau_1, -\infty) = \mathcal{M}(\tau_1)$ (dropping irrelevant phases) and use the simplifications described at the end of Section 3 in this limit.

Number density in an evolved vacuum

Consider a state which at asymptotically early times contained no particles. The expected number of particles (not including antiparticles) with physical momentum $\mathbf{p}^{\text{out}} = \mathbf{p}' = (p^1, p^2, p^3 + eA(t))$ in this state at some later time t is given by

$$\frac{N_{\mathbf{p}, \lambda, -\infty}(t)}{V} = |B_{p,p_z}(\tau)|^2$$

As $\tau \rightarrow \infty$ the asymptotic properties of hypergeometric functions [2, 29] imply that:

$$\frac{N_{\mathbf{p}, \lambda, -\infty}(\infty)}{V} = \frac{\cosh(\pi\rho\Delta E) - \cosh(\pi\rho\Delta p_z)}{\cosh(\pi\rho\Delta E) - \cosh(\pi\rho(E_{+\infty} + E_{-\infty}))}$$

Figure 7 shows $\frac{N_{\mathbf{p}, \lambda, -\infty}(t)}{V}$ as a function of p_z^{out} for $a_0 = 1$, $\rho = 10$ and $\tau = -5, 0, 5$ and ∞ . The three curves in each figure are for $\frac{|\mathbf{p}_\perp|}{m} = 0, 0.5$ and 1 . These figures show how particle creation proceeds. Particles are created with small p_z , and are then accelerated by the electric field to take their place in the final ‘bulge’. The RHS of this final bulge comes from particles created at early times, while the LHS comprises particles that were created at late times and have undergone less acceleration since their creation. The height of the peak at the origin in Figure 7 depends on the strength of the electric field at that time, since this peak represents newly created particles. The corresponding distribution of antiparticles is obtained by reversing the sign of p_z^{out} .

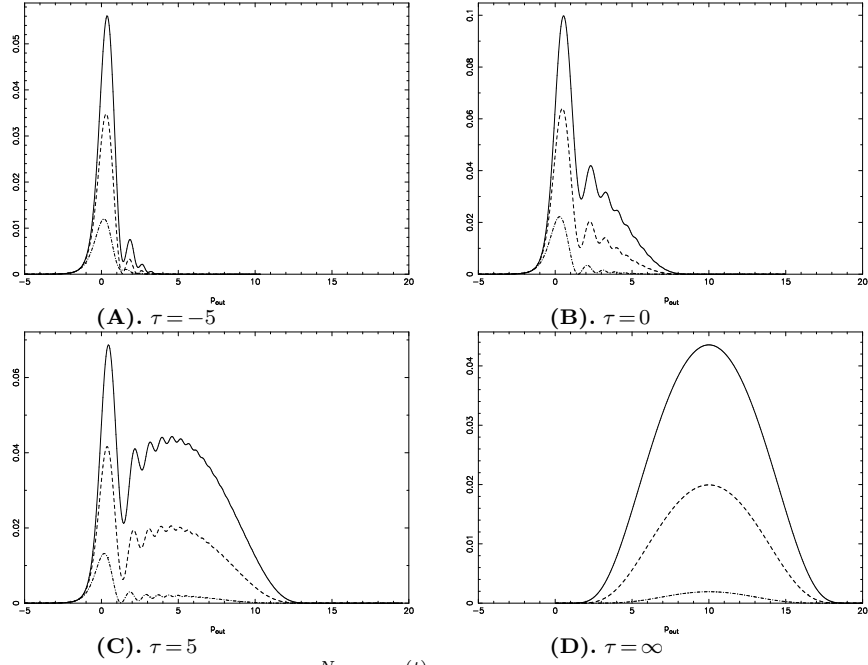


FIG 7. The particle density $\frac{N_{\mathbf{p},\lambda,-\infty}(t)}{V}$ in the evolved ‘in’ vacuum as a function of $\frac{p_{\text{out}}^3}{m}$, for $a_0 = \frac{E}{E_c} = 1$, $\rho = 10$, $\frac{|\mathbf{p}_\perp|}{m} = 0, 0.5$ and 1 , and for $\tau = mt = -5$ (A), 0 (B), 5 (C) and ∞ (D).

Figure 8 shows the total number density of particles in a Compton volume (m^{-3}) of the evolved vacuum, $\frac{N_{\text{vac},-\infty}(\tau)}{Vm^3}$ as a function of τ . This has been evaluated by Monte Carlo sampling over $|p_x| \leq 2$, $|p_y| \leq 2$ and over $|p_z| \leq 8$ (which corresponds to $-3 < p_z^{\text{out}} < 13$). This range is large enough to include the dominant contribution to the integral. The two curves are the result of independent sets of 100,000 samples, giving an idea of the numerical accuracy.

Figure 9 is a repeat of Figure 7 but with $a_0 = \frac{E}{E_c} = 10$ and $\rho = 1$. Particle creation now occurs over a much shorter period of time, so the distinction between the peak at the origin and the late-time bulge is much less pronounced.

To understand this peak at the origin in more detail, examine Figure 10. Here we show $\frac{N_{\mathbf{p},\lambda,-\infty}(t)}{V}$ as a function of τ , for $a_0 = \frac{E}{E_c} = 1$, $\frac{|\mathbf{p}_\perp|}{m} = 0$, $\rho = 5$, and for $p_z = -6$ (A), -3 (B), 0 (C), 3 (D), 6 (E) and ± 40 (F). From (B), (C) and (D), the most significant change in the occupation number of any mode occurs at the time when the covariant momentum of that mode

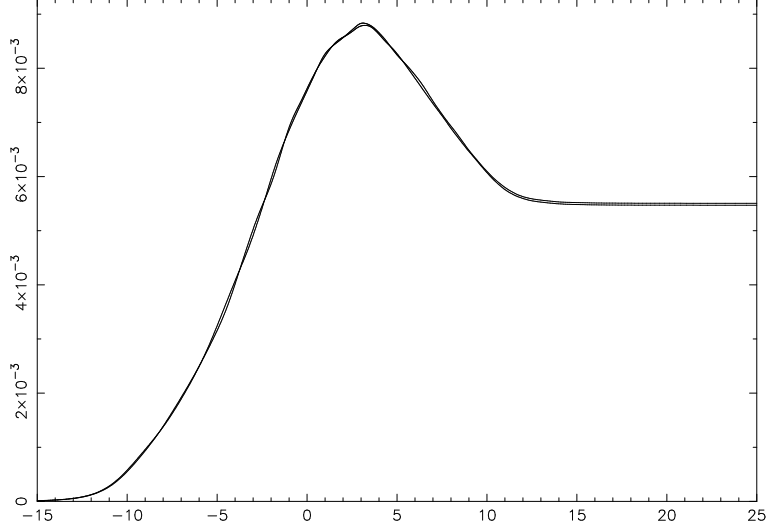


FIG. 8. Monte-Carlo calculation of the total number density of particles in a Compton volume m^{-3} for $a_0 = 1$ and $\rho = 10$.

passes through zero. That is, a mode is most likely to be excited from the Dirac Sea when its momentum passes through zero in the frame of the electric field. If the mode does not pass through zero (as in (A) (E) and (F)) then, although $\frac{N_{\mathbf{p},\lambda,-\infty}(t)}{V}$ can become non-zero during periods when $a(\tau)$ changes so that $E(t)$ is significant, this effect is small and transient. This transient effect is also influenced slightly by the momentum of the relevant mode, with the position of the peak shifted towards times when the momentum was smallest. However, when the relative change in the momentum is small, the peak is displaced much less, and $\frac{N_{\mathbf{p},\lambda,-\infty}(t)}{V}$ more closely resembles $E(t)$.

It is useful to compare Figures such as 7(D) and 9(D) with Figure 11(A). In Figure 11(A) we see that when a_0 is large the bulge becomes much more steep-edged. For $a_0 = 200$ we see that (at least for $|\mathbf{p}_\perp| = 0$) any mode for which p_z^{out} passes through zero will almost certainly be created. Figure 11(B) shows how this result changes upon increasing $|\mathbf{p}_\perp|$. Modes with higher $|\mathbf{p}_\perp|$ require more energy for their creation, hence an increase in $|\mathbf{p}_\perp|$ decreases the number and smoothes the distribution of the created particles.

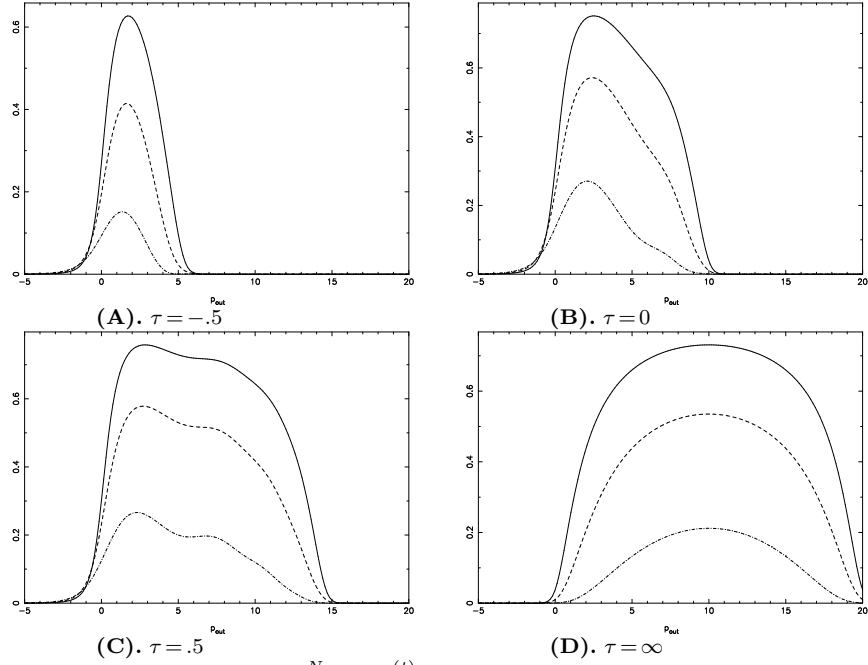
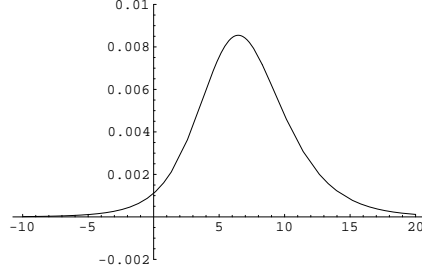


FIG. 9. The particle density $\frac{N_{\mathbf{p},\lambda,-\infty}(t)}{V}$ in the evolved ‘in’ vacuum shown as a function of $\frac{p_{\text{out}}^3}{m}$, for $a_0 = \frac{E}{E_c} = 10$, $\rho = 1$, $\frac{|\mathbf{p}_\perp|}{m} = 0, 1$ and 2 , and for $\tau = mt = -0.5$ (A), 0 (B), $.5$ (C) and ∞ (D).

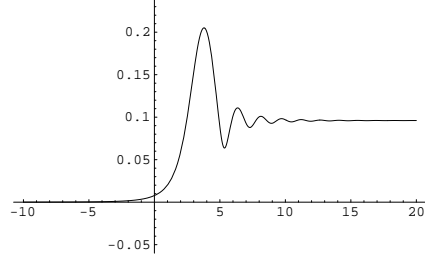
Figure 12 shows the particle density $\frac{N_{\mathbf{p},\lambda,t_0}(t)}{V}$ in an evolved state that was vacuum at time $\tau_0 = mt = -5$ as a function of $\frac{p_{\text{out}}^3}{m}$ for $a_0 = \frac{E}{E_c} = 1$, $\frac{|\mathbf{p}_\perp|}{m} = 0$, and for various ρ and τ . The curves further confirm the present interpretation of the particle creation process. All have a peak at the right hand side (even for $\tau = \infty$), which comes from the initial burst of particle creation, much as in the constant electric field case. The size of this burst is related to the strength of the electric field at time t_0 , such that the graphs in 12(D) are the reflection of $\frac{N_{\mathbf{p},\lambda,-\infty}(t)}{V}$ about $p_z^{\text{out}} = a_0\rho$. Figures (A), (B) and (C) are qualitatively similar to the curves in Figure 2, especially for $\rho = 20$. This is expected, since $a(\tau)$ does not differ significantly from a_0 for $\rho = 20$ $-5 < \tau < 10$.

Current in an evolved vacuum

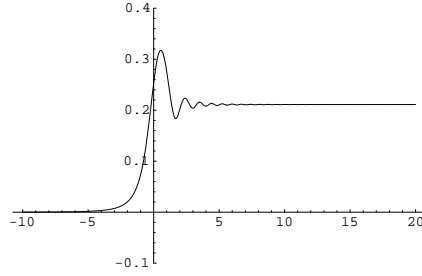
Having seen how the process of particle creation takes place, the predicted current in the evolved vacuum provides no further surprises.



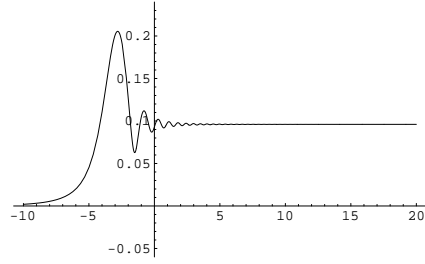
(A). $p_z = -6$. The covariant z -momentum of this mode is always negative.



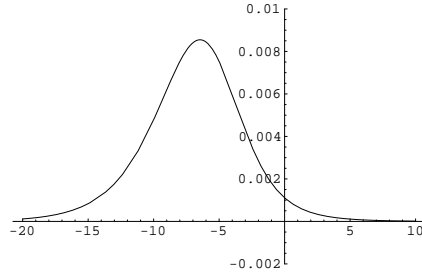
(B). $p_z = -3$. The covariant z -momentum of this mode passes through zero at $\tau \approx 3.47$.



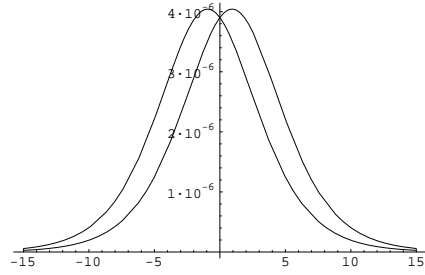
(C). $p_z = 0$. The covariant z -momentum of this mode passes through zero at $\tau = 0$.



(D). $p_z = 3$. The covariant z -momentum of this mode passes through zero at $\tau \approx -3.47$.



(E). $p_z = 6$. The covariant z -momentum of this mode is always positive.



(F). $p_z = \pm 40$. The position of the peak approaches zero as $p_z \rightarrow \pm\infty$.

FIG. 10. The particle density $\frac{N_{\mathbf{p}_{\perp}, -\infty}(t)}{V}$ in the evolved ‘in’ vacuum as a function of τ , for $a_0 = \frac{E}{E_c} = 1$, $\frac{|\mathbf{p}_{\perp}|}{m} = 0$, $\rho = 5$, and for $p_z = -6$ (A), -3 (B), 0 (C), 3 (D), 6 (E) and ± 40 (F).

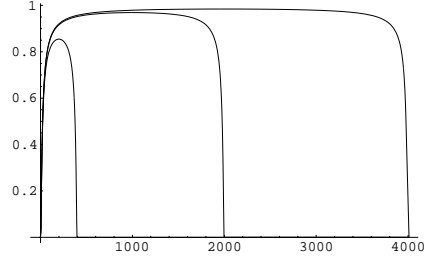


FIG. 11(A). The particle density $\frac{N_{\mathbf{p}, \lambda, -\infty(\infty)}}{\sqrt{V}}$ in the infinitely evolved ‘in’ vacuum shown as a function of $\frac{p_{out}^3}{m}$, for $\rho = 10$, $\frac{|\mathbf{p}_\perp|}{m} = 0$, and $a_0 = \frac{E}{E_c} = 20, 100$ and 200.

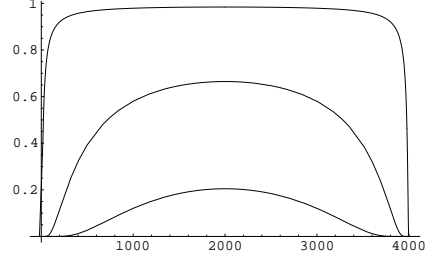
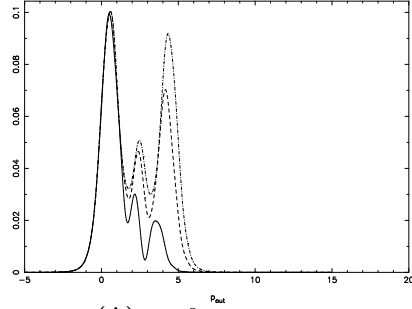
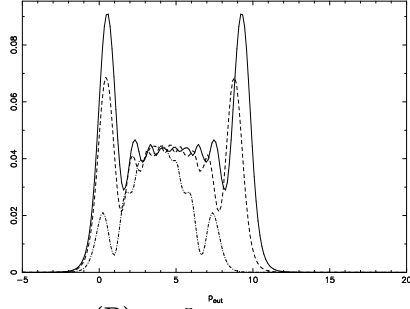


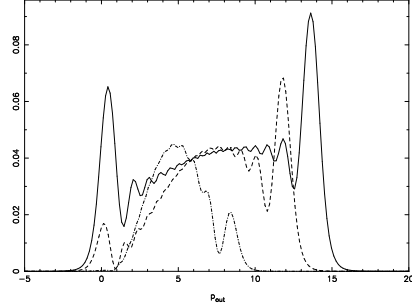
FIG. 11(B). The particle density $\frac{N_{\mathbf{p}, \lambda, -\infty(\infty)}}{\sqrt{V}}$ in the infinitely evolved ‘in’ vacuum shown as a function of $\frac{p_{out}^3}{m}$, for $\rho = 10$, $a_0 = \frac{E}{E_c} = 200$, and $\frac{|\mathbf{p}_\perp|}{m} = 0, 5$, and 10.



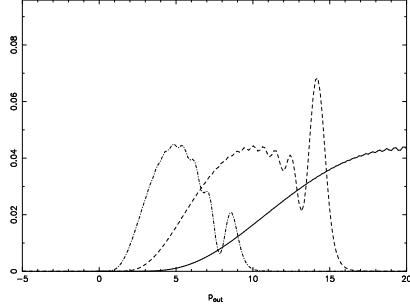
(A). $\tau = 0$



(B). $\tau = 5$



(C). $\tau = 10$



(D). $\tau = \infty$

FIG. 12. The particle density $\frac{N_{\mathbf{p}, \lambda, t_0}(t)}{\sqrt{V}}$ in an evolved state that was vacuum at time $\tau_0 = mt = -5$ shown as a function of $\frac{p_{out}^3}{m}$, for $a_0 = \frac{E}{E_c} = 1$, $\frac{|\mathbf{p}_\perp|}{m} = 0$, $\rho = 5, 10$ and 20, and for $\tau = mt = 0$ (A), 5 (B), 10 (C) and ∞ (D).

Figure 13 shows the integrand of $\frac{J_{vac, 3, -\infty}(t)}{\sqrt{V}}$ as a function of p_z^{out} , for $a_0 = \frac{E}{E_c} = 1$, $\frac{|\mathbf{p}_\perp|}{m} = 0$, $\rho = 5$, and for various τ ; Figure 14 shows the same

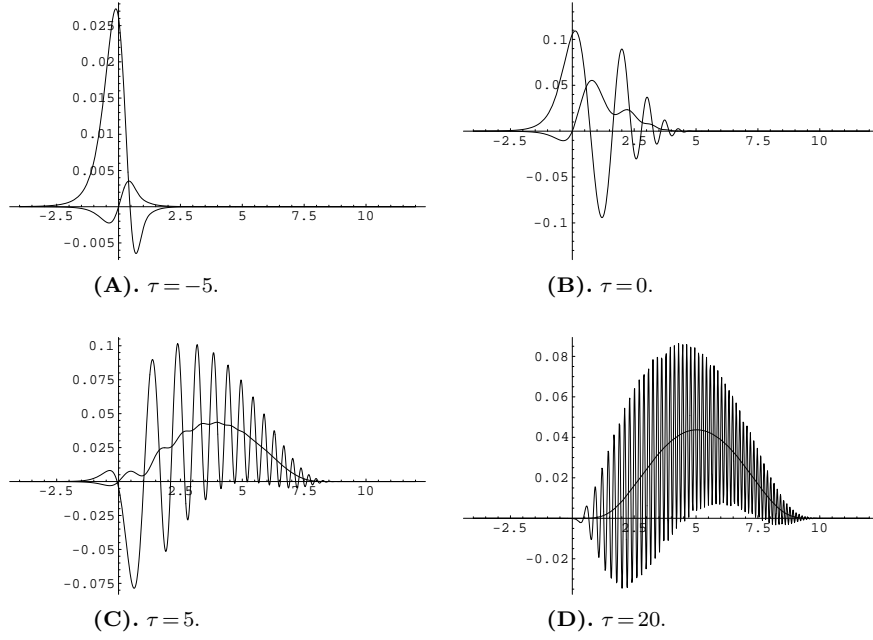


FIG. 13. Current density in the evolved ‘in’ vacuum shown as a function of p_z^{out} for $a_0 = \frac{E}{E_c} = 1$, $\frac{|\mathbf{p}_\perp|}{m} = 0$, $\rho = 5$ and $\tau = -5$ (A), 0 (B), 5 (C) and 20 (D). The $|\beta|^2$ contribution is also shown (the darker curve). The $\Re(\beta\alpha)$ term at late times produces rapid oscillations about the $|\beta|^2$ term, in contrast to early times (as shown in A).

quantity as a function of τ for various p_z . The $|\beta|^2$ contribution has also been included. As in Figure 4, we see that at late times the $\Re(\beta\alpha)$ term simply provides rapid oscillations about the $|\beta|^2$ contribution. Also, the contribution to $\frac{J_{\text{vac},3,-\infty}(t)}{V}$ from the $p_z = 6$ mode is very small in Figure 14. This is because the covariant momentum of this mode never passes through zero.

Figure 15 shows the total current $J_{\text{vac},3,-\infty}(t)$ in a Compton volume m^{-3} of the evolved ‘in’ vacuum, as a function of τ , for $a_0 = 1$ and $\rho = 5$. This current has been evaluated by integrating $J_{\text{vac},3,-\infty}(t)$ over $|p_x| \leq 2$, $|p_y| \leq 2$ and over $|p_z| \leq 8$ (which corresponds to $-3 < p_z^{\text{out}} < 13$). This range is large enough to include the dominant contribution to the integral, but ensures that the cut-off-dependent logarithmic divergence term is small enough to be ignored. By analysing the high-momentum behaviour of the integrand we can confirm the existence of a logarithmic divergence proportional to $\ddot{a}(\tau)$, as expected. The curves are not as smooth as those of Figure 8 because the rapid oscillations have not been completely averaged out.

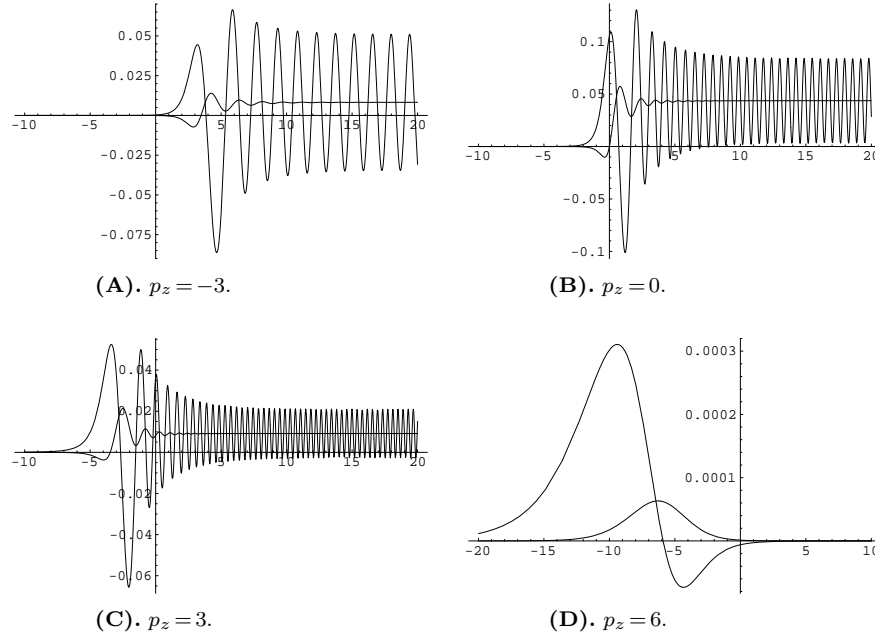


FIG. 14. Current density in the evolved ‘in’ vacuum shown as a function of τ for $a_0 = \frac{E}{E_c} = 1$, $\frac{|\mathbf{p}_\perp|}{m} = 0$, $\rho = 5$ and $p_z = -3$ (A), 0 (B), 3 (C) and 20 (D). The $|\beta|^2$ contribution is also shown (darker curve).

Non-Vacuum initial conditions

Consider now a state which at asymptotically early times contained exactly 1 particle, with momentum \mathbf{p}_{in} . As in Section 4, the current of this state at later times contains two contributions, one from $J_{\text{vac},3,-\infty}(t)$ and one from $J(u\mathbf{p}_{\text{in},\lambda,-\infty}(\mathbf{x},t))$. The z -component of $J(u\mathbf{p}_{\text{in},\lambda,-\infty}(\mathbf{x},t))$ is shown in Figure 16 as a function of τ , for $a_0 = 1$, $\rho = 5$, $|\mathbf{p}_\perp^{\text{in}}| = 0$, and $p_z^{\text{in}} = -8, -5, -2$ and 1. Also included on each graph is the classically expected current for a particle accelerated from rest in this electric field. For (A), (B) and (C) these curves are qualitatively similar to Figure 6, the only difference being that τ now runs from $-\infty$. In Figure 16(D), for which the physical momentum of the mode never passes through zero, the quantum result is indistinguishable from the classical result.

6. CONCLUSIONS

We have applied the particle definition proposed in [13, 14] to the study of particle creation in spatially uniform electric fields. By incorporating

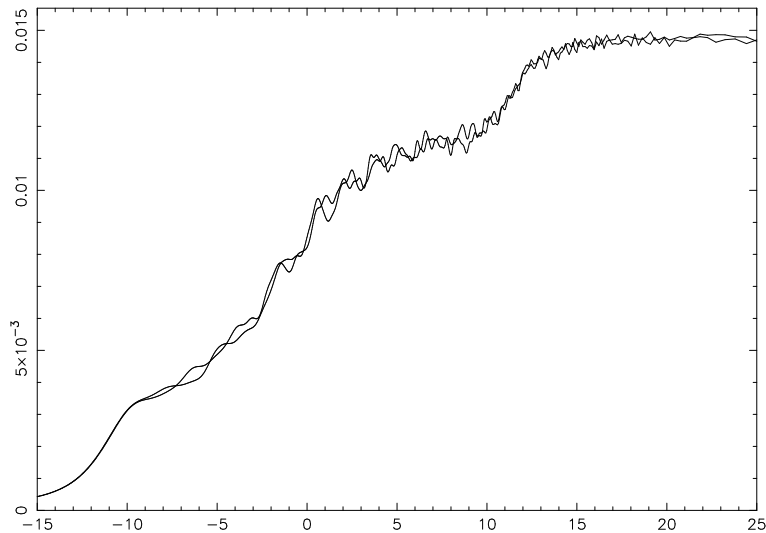


FIG. 15. Monte-Carlo calculation of the total current in a Compton volume m^{-3} for $a_0 = 1$ and $\rho = 10$. The two curves are independent sets of 100,000 samples, giving an idea of the numerical accuracy.

the ‘Bogoliubov coefficient’ and ‘tunnelling’ approaches into a single consistent, gauge-invariant definition, we have resolved several problems raised by Sriramkumar et al. [12, 8]. We have demonstrated the utility of a time-dependent particle interpretation by presenting the time-development of the particle creation process, concentrating on the cases of a time-invariant electric field and an ‘adiabatic’ electric field. For a time-invariant electric field we found, as expected for a first-order linear evolution equation, that the particle content after a finite amount of time T is the same [2, 6] as after evolution of a free ‘in’ vacuum in the presence of a background that was switched on only for a time T . For the adiabatic case we have given a coherent account of the time-development of the particle production process, in which the particles are created with small momentum (in the frame of the electric field), and are then accelerated by the electric field to fill out the ‘bulge’ of created particles predicted by asymptotic calculations [2]. The current in the evolved vacuum is consistent with this picture, although the $\Re(\beta\alpha)$ term corresponds to oscillations around the $|\beta|^2$ term and contains the well-known logarithmic divergence, proportional to $\ddot{a}(t)$. We have also considered an initial state with one particle, and described how this state evolves as the sum of two contributions: the ‘sea of current’ produced by

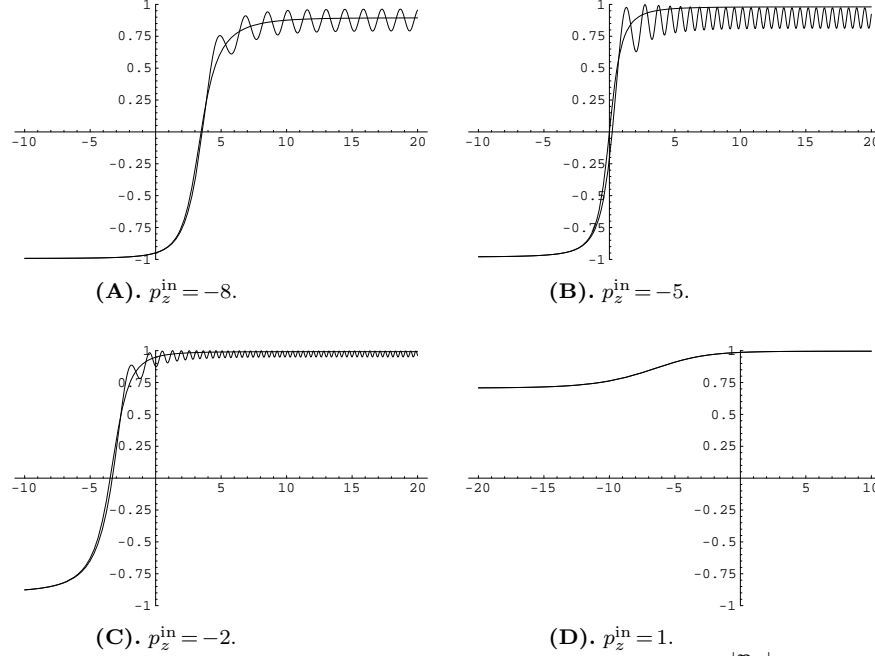


FIG. 16. $J(u_{\mathbf{p}_{\text{in}}, \lambda; t_0}(\mathbf{x}, t_0 + \frac{\tau}{\sqrt{eE}}))$ as a function of τ , for $a_0 = \frac{E}{E_c} = 1$, $\frac{|\mathbf{p}_\perp|}{m} = 0$, $\rho = 5$ and $p_z^{\text{in}} = -8$ (A), -5 (B), -2 (C) and 1 (D). Also included is the current expected classically for a particle accelerated from rest in this electric field.

the evolved vacuum, and the extra current arising from the initial particle state.

The repeated mention of ‘small momentum’ throughout this work may cause concern about the Lorentz covariance of our procedure. In a constant electric field the class of observers moving at constant velocity in the z -direction all measure the same electric field in their rest frame. Can they really all measure the particles to be created with low p_z in their rest frames? Of course they do not all measure this. The reason is hidden in the initial conditions. Insistence that the state be vacuum at time $t = t_0$ effectively chooses a fixed reference frame O . An observer in another frame O' would find no time t' for which the state prepared as above contains no particles. Consequently, no contradiction arises.

We hope this work, along with the formalism presented in [13, 14], has shown the computational and conceptual value of working with a concrete representation of the Dirac Sea. We strongly support Jackiw’s claim [30] that “physical consequences can be drawn from Dirac’s construction”.

ACKNOWLEDGMENTS

We thank Anton Garrett and Dr Emil Mottola for helpful discussions. Carl Dolby also thanks Trinity College and Cavendish Astrophysics for financial support, and thanks the Institute for Nuclear Theory, University of Washington and the Wellcome Trust Centre for Human Genetics, Oxford, for hospitality during his visits.

REFERENCES

1. J. Schwinger, On gauge invariance and vacuum polarisation, *Phys. Rev.* **82**(5) (1951), 664–679.
2. S. P. Gavrilov & D. M. Gitman, Vacuum instability in external fields, *Phys. Rev. D* **53**(12) (1996), 7162–7175.
3. T. Damour, Klein paradox and vacuum polarization, in “Proceedings of The First Marcel Grossmann Meeting on General Relativity,” North-Holland, Amsterdam, 1975.
4. A. I. Nikishov, Pair production by a constant external field, *Soviet Physics JETP* **30**(4) (1970), 660–662.
5. R. Brout, S. Massar, R. Parentani & Ph. Spindel, A primer for black hole physics, *Phys. Rep.* **260** (1995), 329–446.
6. J. Hallin & P. Liljeborg, Fermionic and bosonic pair creation in an external electric field at finite temperature using the functional Schrödinger representation, *Phys. Rev. D* **p52**(2) (1995), 1150–1164.
7. C. Keifer & A. Wipf, Functional Schrödinger equation for Fermions in external gauge fields, *Ann. Phys.* **236** (1994), 241–285.
8. L. Sriramkumar & T. Padmanabhan, Probes of the vacuum structure of quantum fields in classical backgrounds, gr-qc/9903054.
9. L. Sriramkumar, On the response of detectors in classical electromagnetic backgrounds, *Mod. Phys. Lett. A* **14** (1999), 1869–1880.
10. Y. Kluger, J. M. Eisenberg, B. Svetitsky, F. Cooper & E. Mottola, Fermion pair production in a strong electric field, *Phys. Rev. D* **45**(12) (1992), 4659–4671.
11. Y. Kluger, E. Mottola & J. M. Eisenberg, Quantum Vlasov equation and its Markov limit, *Phys. Rev. D* **58** (1998), 125015-1.
12. L. Sriramkumar & T. Padmanabhan, Does a nonzero tunnelling probability imply particle production in time-independent classical electromagnetic backgrounds?, *Phys. Rev. D* **54**(12) (1996), 7599–7606.
13. C. E. Dolby & S. F. Gull, State-space based approach to quantum field theory for arbitrary observers in electromagnetic backgrounds, *Ann. Phys.* In Press.
14. C. E. Dolby, PhD Thesis. Available from http://www.mrao.cam.ac.uk/~clifford/publications/abstracts/carl_diss.html
15. A. A. Grib and S. G. Mamaev, Contribution to the field theory in Friedmann space, *Sov. Journal Of Nuc. Phys.* **10**(6) (1970), 722–725.
16. A. A. Grib and S. G. Mamaev, Creation of matter in the Friedmann model of the universe, *Sov. Journal Of Nuc. Phys.* **14**(4) (1972), 450–452.
17. S. G. Mamaev, V. M. Mostepanenko, and A. A. Starobinskii, Particle creation from the vacuum near a homogeneous isotropic singularity, *Sov. Phys. JETP* **43**(5) (1976), 823–830.

18. A. A. Grib, S. G. Mamayev and V. M. Mostepanenko, Particle creation and vacuum polarisation in isotropic universe, *J. Phys. A: Math. Gen.* **13** (1980), 2057–2065.
19. S. A. Fulling, Remarks on positive frequency and Hamiltonians in expanding universes, *Gen. Rel. and Grav.* **10(10)** (1979), 807–824.
20. W. G. Unruh, Notes on black-hole evaporation, *Phys. Rev. D* **14** (1976), 870–892.
21. E.S. Fradkin, D. M. Gitman & S. M. Shvartsman, “Quantum Electrodynamics with Unstable Vacuum,” Springer-Verlag, 1991.
22. W. Greiner, B. Müller & J. Rafelski, “Quantum Electrodynamics of Strong Fields,” Springer-Verlag, 1985.
23. J. Schwinger, The theory of quantized fields V, *Phys. Rev.* **93(3)** (1953), 615–628.
24. R. Blandford & R. Znajek, Electromagnetic extraction of energy from Kerr black holes, *Monthly Not. of the Roy. Ast. Soc.* **179** (1977), 433–456.
25. V. S. Beskin, Ya. N. Istomin & V. I. Par’ev, The mechanism of filling the magnetosphere of a supermassive black hole with a plasma, *Astronomicheskij Zhurnal* **69(6)** (1992), 1258–1274.
26. A. Erdelyi et al, “Higher Transcendental Functions, Vols 1 and 2,” McGraw-Hill, 1953.
27. C. Itzykson & J. Zuber, “Quantum Field Theory,” McGraw Hill, 1985.
28. S. Habib, Y. Kluger, E. Mottola & J. P. Paz, Dissipation and decoherence in mean field theory, *Phys. Rev. Lett.* **76(25)** (1996), 4660–4663.
29. N. B. Narozhny & A. I. Nikishov, The simplest processes in a pair-producing electric field, *Sov. J. Nucl. Phys.* **11** (1970), 596–598.
30. R. Jackiw, Effects of Dirac’s negative energy sea on quantum numbers, Dirac Prize Lecture, Trieste, 1999. Available at hep-th/9903255.